Article

Cell Reports

Induction of Nitric-Oxide Metabolism in Enterocytes Alleviates Colitis and Inflammation-Associated Colon Cancer

Graphical Abstract

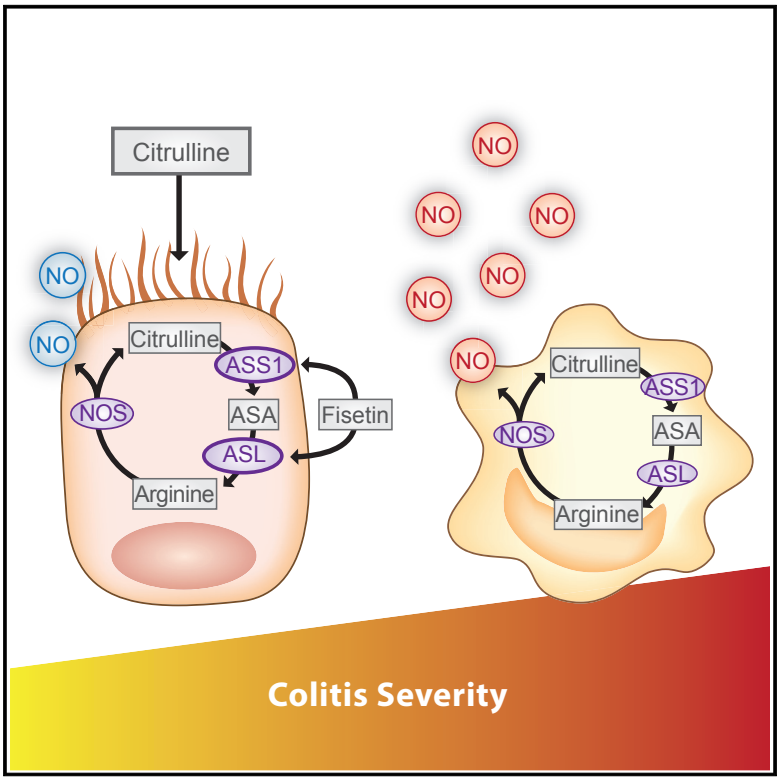

Highlights

- ASL CKO enables dissection of NO contribution to disease in a cell-specific manner
- NO has different roles in the specific cell types relevant to colitis
- NO synthesis in enterocytes is a native defense mechanism against colitis
- Metabolic modulation of NO levels is beneficial for colitis and associated colon cancer

Authors

Noa Stettner, Chava Rosen, Biana Bernshtein, ..., Steffen Jung, Alon Harmelin, Ayelet Erez

Correspondence

ayelet.erez@weizmann.ac.il

In Brief

ASL levels metabolically regulate NO synthesis in a cell-specific manner. Here, we find that cell-autonomous production of NO by enterocytes can be protective as part of the innate immune response against colitis. Finally, we demonstrate the superior advantage of metabolic modulation as a therapy for colitis and inflammation-associated colon cancer.

Stettner et al., 2018, Cell Reports *23*, 1962–1976
May 15, 2018
https://doi.org/10.1016/j.celrep.2018.04.053

CellPress

OPEN ACCESS
CellPress

Cell Reports
Article

Induction of Nitric-Oxide Metabolism in Enterocytes Alleviates Colitis and Inflammation-Associated Colon Cancer

Noa Stettner,[1,2,3] Chava Rosen,[4,5] Biana Bernshtein,[4] Shiri Gur-Cohen,[4] Julia Frug,[1] Alon Silberman,[1] Alona Sarver,[1] Narin N. Carmel-Neiderman,[1] Raya Eilam,[2] Inbal Biton,[2] Meirav Pevsner-Fischer,[4] Niv Zmora,[4] Alexander Brandis,[6] Keren Bahar Halpern,[7] Ram Mazkereth,[8] Diego di Bernardo,[9,10] Nicola Brunetti-Pierri,[9,11] Muralidhar H. Premkumar,[12,13] Gillian Dank,[3] Sandesh C.S. Nagamani,[13,14,15] Steffen Jung,[4] Alon Harmelin,[2] and Ayelet Erez[1,16,*]

[1]Department of Biological Regulation, Weizmann Institute of Science, Rehovot, Israel
[2]Department of Veterinary Resources, Weizmann Institute of Science, Rehovot, Israel
[3]Koret School of Veterinary Medicine, Hebrew University, Rehovot, Israel
[4]Department of Immunology, Weizmann Institute of Science, Rehovot, Israel
[5]The Talpiot Medical Leadership Program, Sheba Medical Center, Tel-Hashomer, Israel
[6]Department of Biological Services, Weizmann Institute of Science, Rehovot, Israel
[7]Department of Molecular Cell Biology, Weizmann Institute of Science, Rehovot, Israel
[8]The Sackler School of Medicine, Tel-Aviv University, Tel-Aviv, Israel
[9]Telethon Institute of Genetics and Medicine, Pozzuoli, Italy
[10]Department of Chemical, Materials and Industrial Engineering, Federico II University, Naples, Italy
[11]Department of Translational Medicine, Federico II University, Naples, Italy
[12]Department of Pediatrics, Baylor College of Medicine, Houston, TX, USA
[13]Texas Children's Hospital, Houston, TX, USA
[14]Department of Molecular and Human Genetics, Baylor College of Medicine, Houston, TX, USA
[15]Department of Medicine, Baylor College of Medicine, Houston, TX, USA
[16]Lead Contact
*Correspondence: ayelet.erez@weizmann.ac.il
https://doi.org/10.1016/j.celrep.2018.04.053

SUMMARY

Nitric oxide (NO) plays an established role in numerous physiological and pathological processes, but the specific cellular sources of NO in disease pathogenesis remain unclear, preventing the implementation of NO-related therapy. Argininosuccinate lyase (ASL) is the only enzyme able to produce arginine, the substrate for NO generation by nitric oxide synthase (NOS) isoforms. Here, we generated cell-specific conditional ASL knockout mice in combination with genetic and chemical colitis models. We demonstrate that NO derived from enterocytes alleviates colitis by decreasing macrophage infiltration and tissue damage, whereas immune cell-derived NO is associated with macrophage activation, resulting in increased severity of inflammation. We find that induction of endogenous NO production by enterocytes with supplements that upregulate ASL expression and complement its substrates results in improved epithelial integrity and alleviation of colitis and of inflammation-associated colon cancer.

INTRODUCTION

Inflammatory bowel disease (IBD), comprised of Crohn's disease and ulcerative colitis, is a chronic inflammation of the digestive tract. Multiple factors, including genetic predisposition, environment, gut microbiota, altered barrier function of the intestinal lining, and dysregulated immune response, are key elements in IBD pathogenesis (Atreya and Neurath, 2015; de Souza and Fiocchi, 2016). Nitric oxide (NO), an important signaling molecule, is a homeostatic regulator of gastrointestinal integrity by maintaining perfusion, epithelial and vascular permeability, and gut motility (Alican and Kubes, 1996; Blaise et al., 2005; Moncada, 1992; Shah et al., 2004). In addition, NO signaling is important for the host immune response and tissue repair (Brown et al., 1993; Witthöft et al., 1998). Although a substantial increase in NO signaling has been implicated in the pathogenesis of human IBD, the specific cellular origin of NO and the exact roles of epithelial and immune cell-derived NO in intestinal inflammation remain unclear (Boughton-Smith et al., 1993; Kolios et al., 2004; Middleton et al., 1993; Suschek et al., 2004). A primary reason for the limited understanding of the role of cell- and context-dependent NO signaling in IBD is the redundancy of the three isoforms of nitric oxide synthase (NOS): endothelial (eNOS), neuronal (nNOS), and inducible (iNOS). The NOS isoforms are often co-expressed in multiple cell types, which prevents dissection of cell-specific NO contributions to disease pathogenesis in both *in vitro* and *in vivo* models (Knowles and Moncada, 1994; Soufli et al., 2016).These obstacles have precluded implementation of NO-related therapies, necessitating a translational model system that overcomes these limitations.

All three NOS isoforms use arginine as a substrate for NO synthesis. Argininosuccinate lyase (ASL), a urea cycle enzyme, is the only mammalian enzyme that can endogenously generate

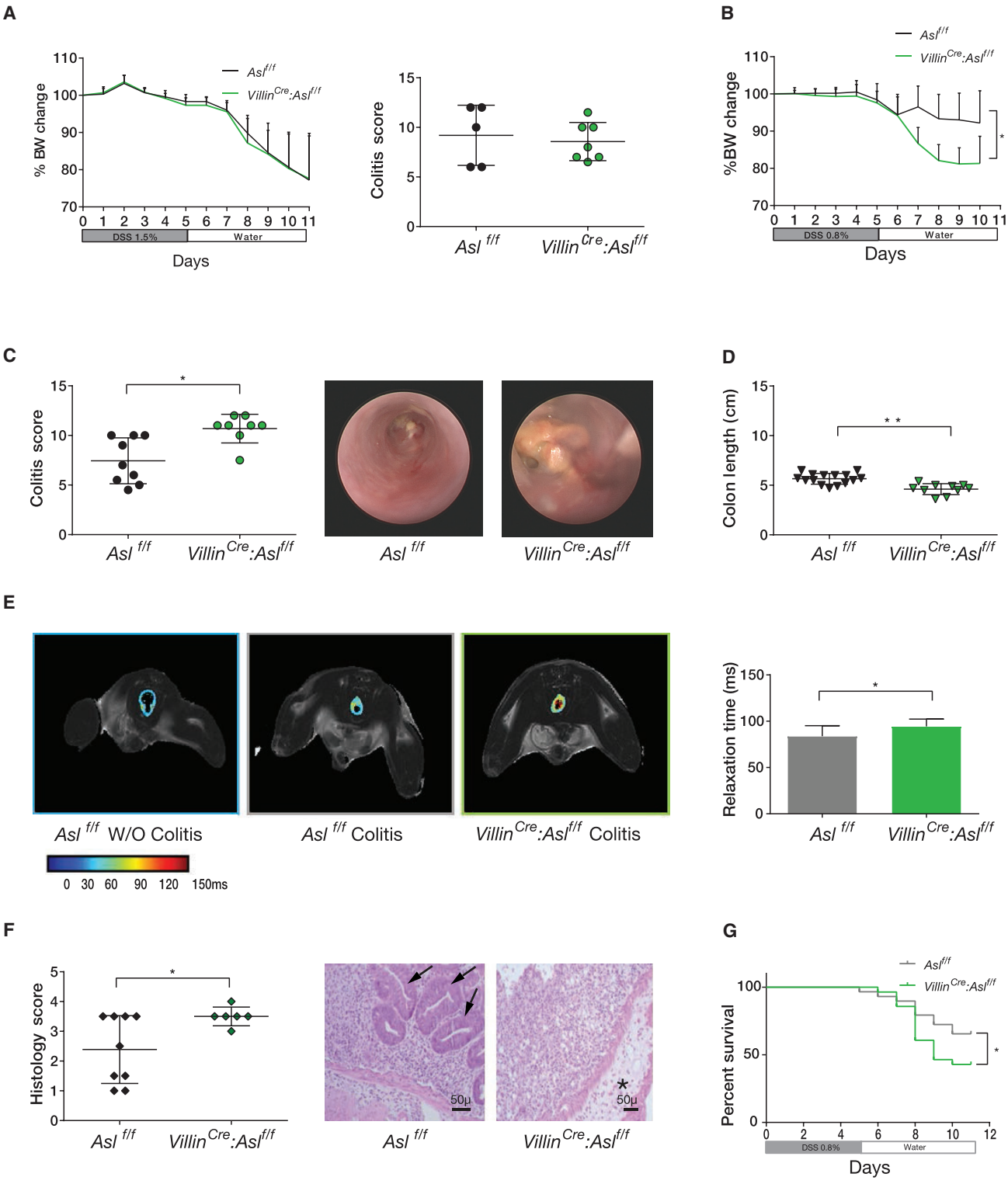

Figure 1. Increased Colitis Severity in ASL CKO Enterocytes

(A) In mice fed an arginine-sufficient diet, there were no noticeable differences in body weight (left) or colitis score (right) between $Asl^{f/f}$ and $Villin^{Cre}:Asl^{f/f}$ mice ($n \geq 5$ in each group, experiments were repeated at least three times).

(legend continued on next page)

arginine. Outside of the liver, ASL, together with another urea cycle enzyme, argininosuccinate synthase (ASS1), participates in the citrulline-arginine cycle, in which arginine is recycled back to citrulline by NOS, which also generates NO in this reaction (Erez et al., 2011a; Nagamani et al., 2012). Because arginine is a semi-essential amino acid, ASL is likely to play a key role in maintaining arginine homeostasis at the tissue level in arginine-deficient states, such as intestinal inflammation (Erez et al., 2011a). We have previously shown that loss of ASL leads to metabolic restriction of arginine for all NOS-derived NOs (Erez et al., 2011b). Here we use models with cell-specific loss of ASL to better understand the cell-specific contributions of NO in the causation of IBD.

RESULTS

Generating Cell-Specific Impairment of Arginine Production in Epithelial and Immune Cells and Induction of Colitis

To generate cell-specific conditional ASL knockout (CKO) mice, we crossed $Asl^{f/f}$ animals (Erez et al., 2011b) to three different transgenic mice expressing Cre recombinase under the enterocyte-specific Villin promoter (Madison et al., 2002), the hematopoietic Vav1 promoter (Ogilvy et al., 1998), and the macrophage/dendritic cell (DC)-specific CD11c promoter (Caton et al., 2007; Vander Lugt et al., 2014; Figures S1A–S1F). At baseline, all CKO mice were indistinguishable from their wild-type (WT) littermates and showed no observable phenotype; in particular, there were no differences in blood counts, body weight, arginine levels, and intestinal histology (data not shown; Figures S1E, S1G, and S2A). The severity of intestinal inflammation after induction of colitis was assessed comprehensively by endoscopy, histology, and MRI as well as by evaluating clinical parameters such as weight and survival. In all experiments, $Cre^{-/-}Asl^{f/f}$ littermate mice (labeled $Asl^{f/f}$) were used as controls.

Loss of ASL in Enterocytes Is Detrimental in Arginine-Deficient States

In human and murine enterocytes, expression of ASL is maximal in the second week of life, when the intestine is the principal site of arginine synthesis (De Jonge et al., 1998). In contrast, enterocyte expression of ASL in adult mice is rather limited and thus, expectedly, was not different compared with ASL expression in $Villin^{Cre}:Asl^{f/f}$ mice (Figure S2A). In agreement with ASL expression levels, plasma arginine levels were similar between $Villin^{Cre}:Asl^{f/f}$ adult mice and controls (Figure S1G). Colitis was induced in the CKO models chemically by using dextran sulfate sodium (DSS) (Whittem et al., 2010; Cooper et al., 1993). Following acute colitis induction, ASL levels in control enterocytes were not elevated significantly, and the severity of DSS-induced colonic inflammation was similar in controls and $Villin^{Cre}:Asl^{f/f}$ mice (Figure 1A; Figure S2B). These results are consistent with our previous work showing increased incidence of necrotizing enterocolitis in $Villin^{Cre}:Asl^{f/f}$ mice only in the neonatal period, when there is a significant expression of ASL in enterocytes (Premkumar et al., 2014). In an attempt to generate significant differential ASL expression in adult enterocytes of $Villin^{Cre}:Asl^{f/f}$ mice and control littermates, mice were maintained on an arginine-free diet. As previously described, the weight of these mice was 20% lower than that of the respective genotypes fed an arginine-sufficient diet (Marini et al., 2015). Importantly, dietary arginine restriction resulted in expression of ASL in the intestines of control mice but not in the $Villin^{Cre}:Asl^{f/f}$ animals, although no differences in the animal growth curves or immune infiltrates to the intestine were observed between CKO mice and controls (Figure S1G). Collectively, these results suggest that ASL induction in the adult mouse gut is a physiological mechanism to restore arginine homeostasis during arginine-deficient states.

With an arginine-free diet, induction of colitis with the standard dose of 1.5% DSS was lethal in the $Villin^{Cre}:Asl^{f/f}$ mice (data not shown), necessitating that a lower dose of DSS (0.8%) be used for all experiments. Even with such a reduced DSS challenge, the increased severity of colitis in the $Villin^{Cre}:Asl^{f/f}$ mice compared with controls was evidenced by greater weight loss, increased colonic inflammation, decreased colon length, decreased intestinal relaxation time in MRI (a surrogate marker of inflammation; Martin et al., 2005), a higher histology score, and decreased survival (Figures 1B–1G). To confirm that the enterocyte-specific loss of ASL also increases colitis severity in an independent IBD model, we induced colitis in $Asl^{f/f}$ and $Villin^{Cre}:Asl^{f/f}$ mice by irradiation and engraftment with $CX_3CR1^{Cre}:Il10ra^{f/f}$ donor bone marrow (BM). Specifically, we had previously shown that macrophage-specific deletion of the receptor for the anti-inflammatory cytokine interleukin-10 (IL-10) results in spontaneous and chronic gut inflammation (Glocker et al., 2009; Zigmond et al., 2014). In an extension of this model, lethally irradiated WT animals that received a BM graft from $CX_3CR1^{Cre}:Il10ra^{f/f}$ mice developed spontaneous colitis; hence, this procedure was used by us to generate a genetic model for IBD (Figure S2C). Similarly to DSS-induced colitis, on an arginine-free diet, colitis driven by pro-inflammatory IL-10R-deficient macrophages in $Villin^{Cre}:Asl^{f/f}$ mice was exacerbated compared with controls, as evident by higher colitis and histology scores and decreased

(B–D) Colitis was induced by DSS in $Villin^{Cre}:Asl^{f/f}$ and control $Asl^{f/f}$ mice fed an arginine-free diet. $Villin^{Cre}:Asl^{f/f}$ mice had increased colitis severity compared with control mice as demonstrated by (B) a significantly weight loss (n = 18 in each group), (C) a higher endoscopic colitis score (the right shows a representative colonoscopy image for an experiment with $n \geq 8$ in each group), and (D) shorter colons.

(E) A T2 map of colon section MRI showing increased relaxation time, a marker of inflammation in $Villin^{Cre}:Asl^{f/f}$ compared with control mice. The color gradient ranges from blue, which represents short relaxation, to red, which represents a longer relaxation time, correlating with more severe colon damage. The quantification graph of the images on the right shows a statistically significant increase in relaxation time in CKO enterocytes (n = 11 in each group).

(F) Left: a higher histological score in the $Villin^{Cre}:Asl^{f/f}$ mice ($n \geq 6$ in each group). Right: a representative colon cross-section stained with H&E, showing severe edema and destruction of colon crypts in $Villin^{Cre}:Asl^{f/f}$ mice. The asterisk indicates an area of severe edema. Arrows indicate crypts present in the colon of $Asl^{f/f}$ mice only.

(G) Kaplan-Meier curve showing a higher mortality rate in $Villin^{Cre}:Asl^{f/f}$ mice compared with controls.

Error bars represent SEM.

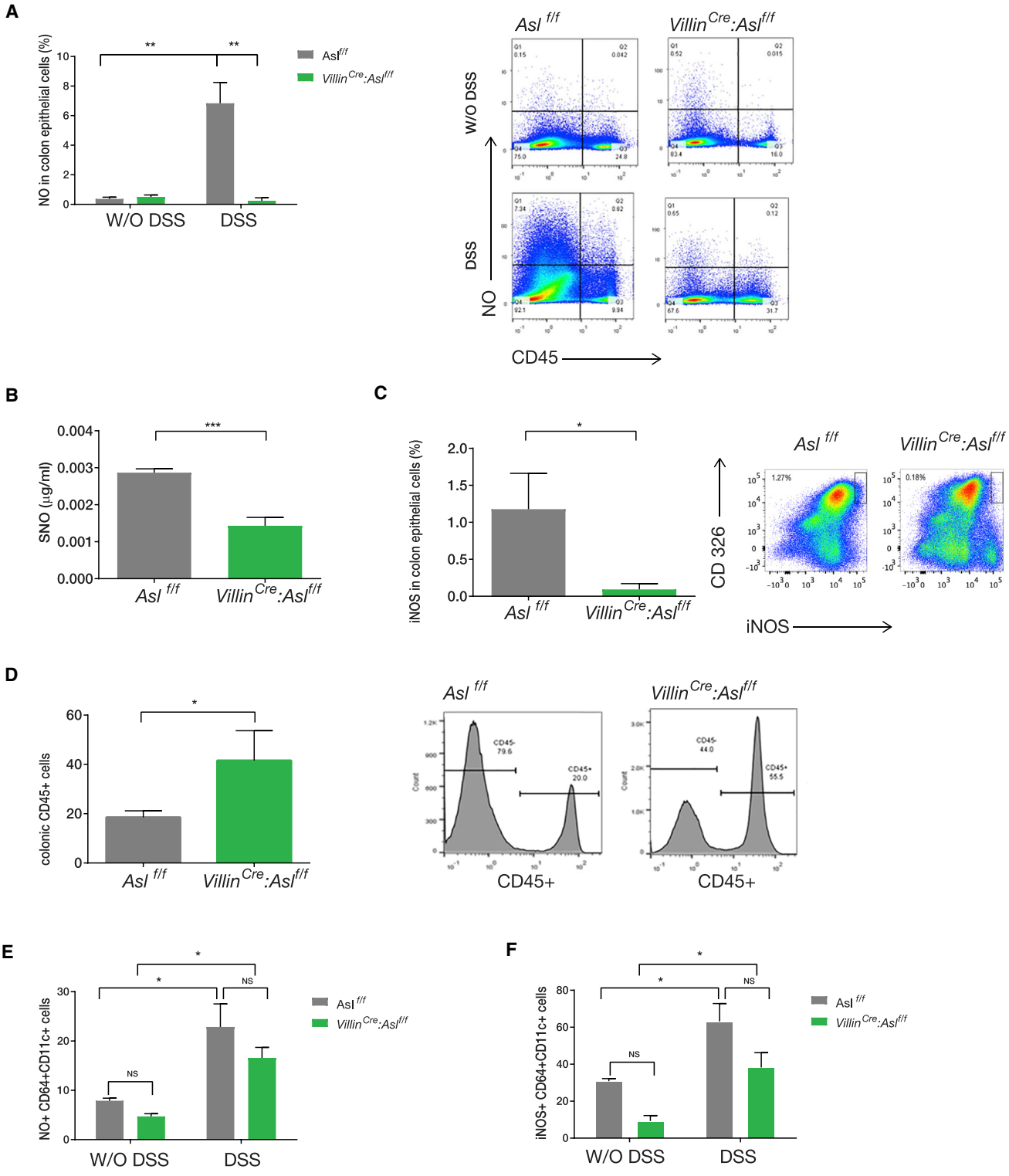

Figure 2. Decreased NO Levels in Enterocytes Increases Colitis Severity

Shown is cell-specific analysis of colon cells from *Villin*^{Cre}*:Asl*$^{f/f}$ and control *Asl*$^{f/f}$ mice before and 10 days after colitis induction by DSS.

(A) CD45− cells fluorescence-activated cell sorting (FACS) analysis shows a significant increase in NO levels in the control group after colitis induction compared with *Villin*^{Cre}*:Asl*$^{f/f}$ mice using 4-amino-5-methylamino-2',7'-difluorofluorescein (DAF-FM) (n = 3 in each group).

(B) ELISA of S-nitrosocysteine expression by CD45– cells (i.e., non-hematopoietic cells), showing no significant increase in nitrosylation after colitis induction in *Villin*^{Cre}*:Asl*$^{f/f}$ mice.

(legend continued on next page)

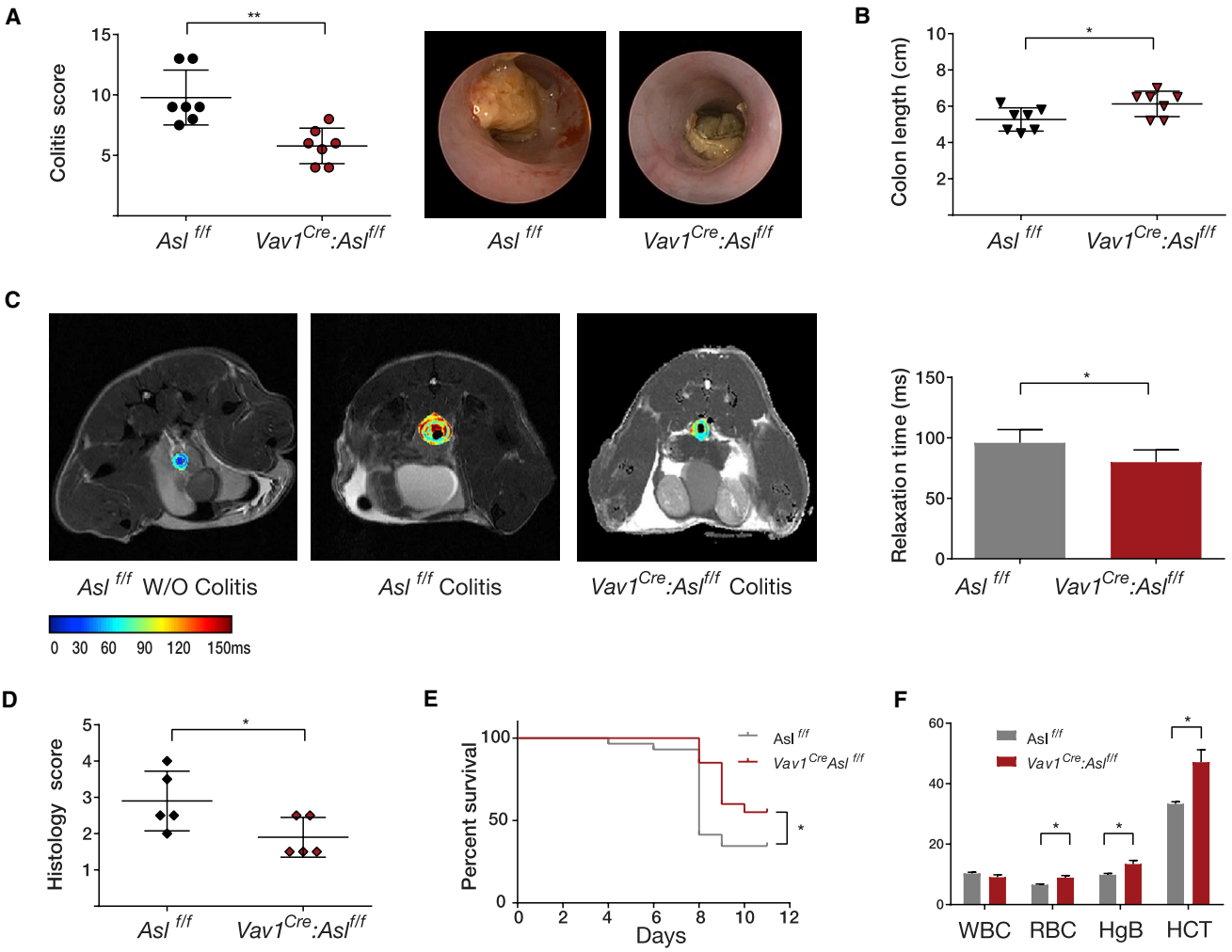

Figure 3. Reduced Colitis Severity in ASL CKO Immune Cells

Colitis was induced by DSS in *Vav1*^{Cre}: *Asl*$^{f/f}$ and in control *Asl*$^{f/f}$ mice.

(A) A representative graph of endoscopic evaluation scores on day 12 after colitis induction, showing a significant improvement in the colitis score of the *Vav1*^{Cre}: *Asl*$^{f/f}$ group compared with the control group. The experiment was performed 3 times with a total of n ≥ 20 mice in each group with 3 repetitions. Right: a representative image of the colon taken by colonoscopy.

(B) A representative experiment showing a significant increase in colon length in *Vav1*^{Cre}: *Asl*$^{f/f}$ mice compared with the control group. The experiment was performed three times with a total of n ≥ 19 mice in each group.

(C) A T2 map of representative colon sections, demonstrating increased relaxation time in the control group compared with *Vav1*^{Cre}: *Asl*$^{f/f}$ mice. Right: quantification of the images using Image-pro Pulse software. The experiment was performed on a total of n = 5 mice in each group.

(D and E) A significant reduction in histological score (D) and a lower mortality rate (E) in *Vav1*^{Cre}: *Asl*$^{f/f}$ mice compared with controls.

(F) Anemia developed only in the control group after colitis induction, as shown by decreased red blood cells (RBCs), hemoglobin (HgB), and hematocrit (HCT) levels. No differences between groups were detected in the white blood cell (WBC) count (n = 3 in each group).

Error bars represent SEM.

colon length (Figure S2D). These results, using two distinct models, suggest that colitis severity is at least in part governed by arginine availability, specifically in enterocytes during arginine-deficient states.

The Increased Colitis Severity Associated with ASL Loss in Enterocytes Is Mediated by NO

Although plasma arginine levels were similar, the combination of an arginine-restricted diet and colitis induction resulted

(C–F) FACS analysis.

(C) A significant increase in iNOS expression in CD45− CD326+ (i.e., colonic enterocytes) in the control group but not in the *Villin*^{Cre}:*Asl*$^{f/f}$ mice after colitis induction.

(D) Increased recruitment of CD45+ immune cells to the colon of *Villin*^{Cre}:*Asl*$^{f/f}$ mice compared with control.

(E and F) A similar upregulation of NO (E) and iNOS (F) in CD64+; CD11c+ colon macrophages in *Villin*^{Cre}:*Asl*$^{f/f}$ mice and in the control group.

Error bars represent SEM.

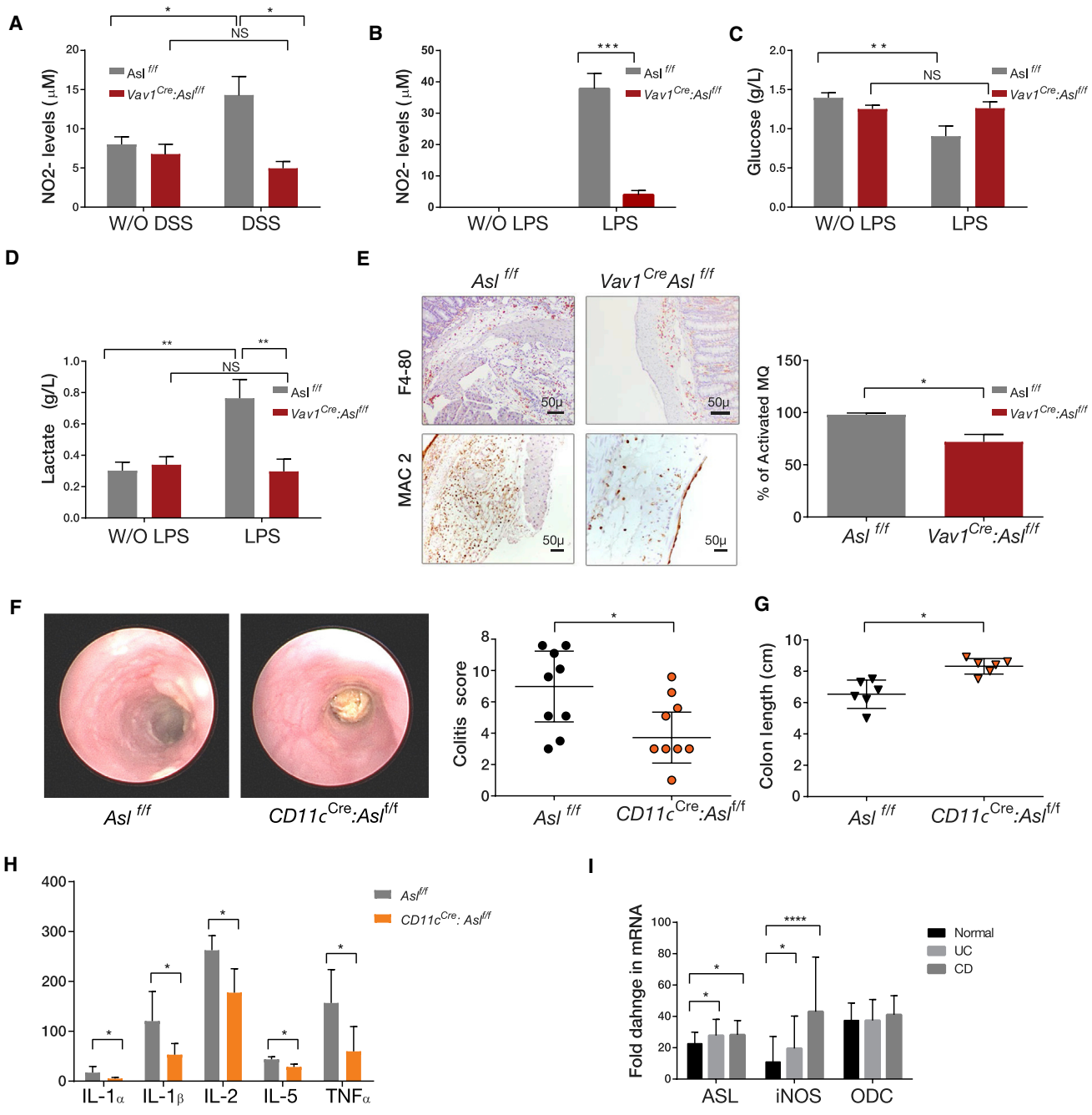

Figure 4. Decreased NO Levels in ASL CKO Immune Cells

(A) Nitrite (NO_2^-) levels were measured by dedicated high-performance liquid chromatography (HPLC) in blood samples before and after colitis induction. Results show a significant elevation in NO levels after colitis induction in RBCs of the control group but not in *Vav1*^{Cre}: *Asl*$^{f/f}$ mice ($n \geq 3$ in each group).

(B) A significant elevation in NO_2^- levels is seen in peritoneal macrophages growth medium 18 hr following LPS administration in the control group compared with the *Vav1*^{Cre}: *Asl*$^{f/f}$ group (n = 6 in each group).

(C and D) A significant reduction in glucose levels (C) and elevation in lactate levels (D) in response to LPS administration is demonstrated in control but not in *Vav1*^{Cre}: *Asl*$^{f/f}$ macrophages. Measurements were performed using a NOVA measuring instrument, ($n \geq 4$ in each group).

(E) Immunohistochemistry staining for the total number of macrophages (using the F4-80 marker, top) as well as for activated macrophages (using the MAC2 marker of activation, bottom), in distal colon sections after colitis induction. The ratio between F4-80- and MAC2-positive cells shows a significant reduction in the number of activated macrophages in *Vav1*^{Cre}: *Asl*$^{f/f}$ mice compared with controls. Cells were counted from at least 8 microscopic fields taken from 3 different animals. Right: quantification analysis.

(F and G) Colitis was induced by DSS in *CD11c*^{Cre}:*Asl*$^{f/f}$ and in control *Asl*$^{f/f}$ mice.

(legend continued on next page)

in significantly reduced arginine levels in enterocytes of *Villin^{Cre}:Asl$^{f/f}$* mice (Figure S2E). This suggested that cell-specific deficiency of arginine, and potentially one of its downstream metabolites, could be enhancing inflammation severity. Because arginine is also the substrate for polyamine synthesis via ornithine, and because polyamines have been shown to play a role in colitis (Coëffier et al., 2010; Rath et al., 2014), we measured the intestinal levels of these metabolites as well and found no significant difference between *Villin^{Cre}:Asl$^{f/f}$* and control mice in the levels of spermidine and spermine or in the spermidine/spermine ratio, which was found to be critical for normal growth and development (Pegg, 2016; Figure S2F). Importantly, sequence analysis confirmed that, on an arginine-free diet without colitis induction, there were no significant differences in microbiome composition between *Villin^{Cre}:Asl$^{f/f}$* mice and controls (Figure S3). Because we had previously shown a critical role for ASL in NO metabolism (Erez et al., 2011b), we next investigated whether enterocyte-specific arginine deficiency leads to decreased NO synthesis by measuring nitrite, an established NO biomarker (Mian et al., 2013), 10 days after colitis induction. This time point was chosen because, with DSS-induced colitis, the intestine is in the post-inflammatory regenerative phase (Whittem et al., 2010), and, thus, nitrite measurements from intestinal homogenates are expected to be more representative of NO production from enterocytes rather than immune cell infiltrates. We found, in enterocytes of *Villin^{Cre}:Asl$^{f/f}$* mice, significantly decreased NO levels as well as reduced nitrosylation and decreased iNOS levels, likely because of the specific decrease in arginine levels (Figures 2A–2C). Simultaneously, during colitis, there was increased recruitment of CD45+immune cells to the intestine of *Villin^{Cre}:Asl$^{f/f}$* animals (Figure 2D). Of note, recruited monocytes/macrophages in *Villin^{Cre}:Asl$^{f/f}$* mice were phenotypically similar to cells infiltrating the intestine of controls because they were able to upregulate iNOS expression and generate NO in response to DSS at comparable levels (Figures 2E and 2F). These results highlight the requirement of arginine by enterocytes during colitis for NO synthesis and allude to the possibility that enterocyte-restricted NO deficiency might contribute to immune cell recruitment to the gut and, hence, exacerbate inflammation.

Reduced NO Production and Colitis Severity in Mice with Immune Cell-Specific ASL Deficiency

Because immune cells were found to have detectable levels of ASL even during basal conditions, no dietary intervention was necessary to reveal differential ASL expression between *Vav1^{Cre}: Asl$^{f/f}$* mice and controls; thus, mice were given a regular diet (Figure S1D). Following colitis induction by a standard dose of DSS (1.5%–2.5%), the degree of colonic inflammation was significantly milder in *Vav1^{Cre}: Asl$^{f/f}$* mice compared with control littermates (Figures 3A–3E). In addition, although control mice had decreased hemoglobin levels following colitis, *Vav1^{Cre}: Asl$^{f/f}$* mice displayed normal hemoglobin levels, likely reflecting decreased blood loss to the stool (Figure 3F). Hence, modulation of ASL levels in a cell type-specific manner differentially affects colitis severity; although ASL produced by enterocytes appears to have a protective role, ASL expression in immune cells exacerbates colonic injury.

Increased NO production by immune cells is a well-known phenomenon associated with inflammation (Eiserich et al., 1998; Guzik et al., 2003; Kolios et al., 2004). In addition, it was recently shown that red blood cells (RBCs) control systemic NO bioavailability by synthesizing, transporting, and releasing NO metabolic products (Cortese-Krott and Kelm, 2014). Indeed, following colitis induction, we found a robust increase in nitrite production by RBCs only in control mice and not in *Vav1^{Cre}: Asl$^{f/f}$* animals (Figure 4A). To confirm that the effect on the inflammatory cascade is caused specifically by decreased NO production by the immune cells of the mutant mice, we conducted *ex vivo* studies with peritoneal macrophages isolated from the *Vav1^{Cre}: Asl$^{f/f}$* mice, the major immune cell type producing NO (Lorsbach et al., 1993), and measured their response to lipopolysaccharide (LPS). Similar to the finding at the whole-organism level, *Vav1^{Cre}:Asl$^{f/f}$* macrophages produced less nitrite in response to LPS (Figure 4B). Lately, several studies have shown that, in addition to the paracrine effects of macrophage-derived NO on other cells, NO has an autocrine effect in polarizing macrophages toward a pro-inflammatory (or "M1") state. The metabolic mechanism behind this phenomenon was proposed to be a prominent induction of glycolysis (Kelly and O'Neill, 2015; Vatassery et al., 2004). We hence measured lactate and glucose levels in the medium of cultured peritoneal macrophages as a readout for macrophage activation (Bustos and Sobrino, 1992). Although macrophages of control mice showed decreased glucose levels and increased lactate production, consistent with increased glycolysis, no such changes were observed in *Vav1^{Cre}: Asl$^{f/f}$* macrophages, suggesting their decreased activation (Figures 4C and 4D). Furthermore, colon histology after induction of colitis revealed decreased recruitment of activated monocytes/macrophages to the intestine in immune *Asl* CKO mice, as demonstrated by a decreased ratio between the general number of macrophages (marked with F-4/80) and the number of activated macrophages (marked with MAC-2) (Rosenberg et al., 1991; Figure 4E). To specifically investigate intestinal

(F) Right: a representative graph showing that *CD11c^{Cre}:Asl$^{f/f}$* mice have decreased colitis severity compared with control mice, as demonstrated by endoscopic evaluation on day 12 after colitis induction. The experiment was performed on a total of $n \geq 13$ mice in each group. Left: a representative image of the colon taken by colonoscopy.

(G) A representative graph showing a significant increase in colon length in *CD11c^{Cre}:Asl$^{f/f}$* mice compared with the control group. The experiment was performed on a total of $n \geq 10$ mice in each group.

(H) ELISA measurement of colon tissues extracted from mice on day12 following colitis induction, showing significant elevation of pro-inflammatory cytokine levels in the control group compared with *CD11c^{Cre}:Asl$^{f/f}$* mice.

(I) Human data taken from a GEO dataset analysis (GEO: GSE57945; ID:200057945), showing significant upregulation of *ASL* and *iNOS* RNA expression in patients suffering from Crohn's disease (CD) and ulcerative colitis (UC) compared with controls, with no significant change in ornithine decarboxylase (ODC) expression.

Error bars represent SEM.

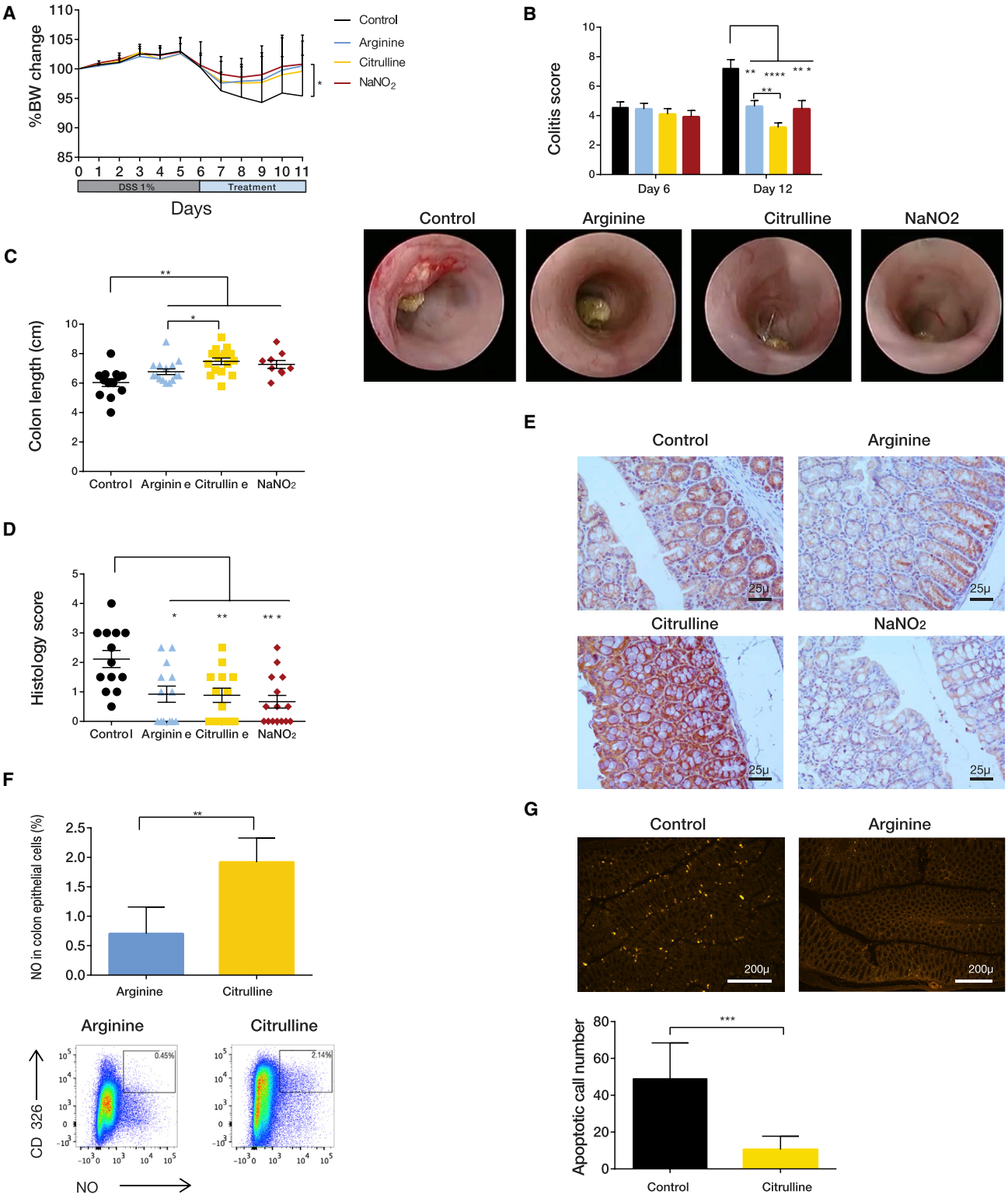

Figure 5. NO-Related Metabolites Alleviate Colitis Severity

Treatment with arginine pathway-related metabolites leads to a significant improvement in colitis severity. Colitis was induced in wild-type C57BL/6J.OlaHsd mice. Mice were treated with DSS for 6 days, followed by administration of either arginine solution in drinking water, citrulline, or $NaNO_2$ or with water as a control for an additional 6 days.

(legend continued on next page)

macrophages, we analyzed the levels of iNOS and NO in gut hematopoietic cells (CD45+) and enterocytes (CD326+) (King et al., 2012). As expected, we found ASL levels to be significantly lower in intestinal CD45+ cells of *Vav1^{Cre}:Asl$^{f/f}$* mice, correlating with decreased iNOS expression and decreased NO production; in contrast, there were no significant differences in these parameters in enterocytes of the same animals (Figures S4A–S4F). To corroborate these results, we generated *CD11c^{Cre}:Asl$^{f/f}$* mice and induced DSS colitis in these animals. Challenged *CD11c^{Cre}:Asl$^{f/f}$* mice displayed a decrease in weight loss, colitis scores, and pro-inflammatory cytokines and an increase in colon length, all supporting ameliorated colitis (Figures 4F–4H). Collectively, our data suggest that loss of ASL in enterocytes has a significant effect on increasing the severity of inflammation, whereas loss of ASL in immune cells, and in particular CD11c^{+} mononuclear phagocytes, alleviates colitis severity, likely because of alterations in NO levels. Interestingly, analysis of the GEO database revealed that *ASL* expression is increased in chronic IBD patients with Crohn's disease or ulcerative colitis compared with controls. Moreover, in contrast to the expression of the rate-limiting enzyme in polyamine synthesis (i.e., ornithine decarboxylase [*ODC*]), *ASL* expression correlates with *iNOS* expression (Figure 4I; Figure S4J). These data provide further support for our assumption of the importance of ASL re-expression in enterocytes during colitis for NO synthesis and for the potential relevance of our findings to human IBD.

Inducing Endogenous NO Production by Enterocytes Alleviates Colitis and Inflammation-Associated Colon Cancer

To investigate whether enhancing NO production can alleviate colitis severity, we induced colitis in WT mice and, 6 days later, examined the response to different NO-related drug interventions. Mice were supplemented with either arginine or citrulline to support NOS-dependent NO generation or with sodium nitrite, an NOS-independent NO supplement. All three interventions led to significant colitis amelioration, as evaluated by change in weight, endoscopy score, colon length, and histology score (Figures 5A–5D). Among these interventions, citrulline induced ASL expression the most (Figure 5E), likely because it metabolically drives ASL activity by increasing its substrate (Wijnands et al., 2012). Furthermore, intestines of mice treated with citrulline showed increased NO generation by enterocytes and decreased apoptosis, correlating with decreased colitis severity (Figures 5F and 5G). Thus, we sought to further investigate the enterocyte-specific induction of ASL and NO using citrulline.

To boost *ASL* expression directly, we performed a screen for Food and Drug Administration (FDA)-approved small molecules that increase *ASL* transcription using the non-biased computational method Mantra, which has been previously developed by us (Iorio et al., 2010). In several cancer cell lines, the flavanol molecule fisetin (3,7,3′,4′-tetrahydroxyflavone) was found to significantly upregulate the RNA expression levels of *ASS1* and *ASL*, which are both required for arginine synthesis from citrulline (Table S1). Fisetin is commonly found in many fruits and vegetables and has been shown to have an anti-inflammatory property (Sahu et al., 2016). We hence aimed to understand its specific effect on enterocytes. Encouragingly, *in vivo* supplementation with fisetin upregulated ASL and ASS1 expression in enterocytes (Figure 6A). Moreover, ASL induction correlated with increased iNOS expression and NO production levels specifically in enterocytes (Figures 6B and 6C; Figures S5A–S5F). Importantly, fisetin therapy alleviated colitis severity in WT mice with respect to all parameters compared with NO donors; however, the compound had no effect in *Villin^{Cre}:Asl$^{f/f}$* mice harboring the enterocyte-specific ASL deficiency. This establishes that it is the specific upregulation of ASL in the intestinal epithelium that is ameliorating colitis (Figures 6D–6F).

Finally, because citrulline is the upstream metabolic substrate for ASS1, we expected that combining citrulline with fisetin would have a synergistic effect. Indeed, supplementing WT mice on a regular diet with fisetin together with citrulline was the most effective modality to generate NO in enterocytes in both the chemically and genetically induced colitis models (Figures 7A–7F). Improved epithelial integrity following increased NO production by fisetin and citrulline in the genetic model of colitis was corroborated by significantly decreased plasma levels of fluorescein isothiocyanate (FITC)-conjugated dextran (Figure 7G). To confirm the human relevance of our findings, we measured conductivity in Caco-2 human epithelial cells (Araki et al., 2006) following exposure to DSS and different drug regimens. In support of our conclusions from the mouse models, we found that the combined treatment improved conductivity, reflecting preservation of the epithelial barrier (Sambuy et al., 2005; Figure 7H).

Because colitis severity has been shown to predispose to colon cancer development (Barral et al., 2016), we used the DSS-azoxymethane (AOM) model for colitis-associated cancer (Thaker et al., 2012). Although there was no significant difference in cancer severity between *Asl$^{f/f}$* and *Vav1^{Cre}*: *Asl$^{f/f}$* (data not shown), *Villin^{Cre}*: *Asl$^{f/f}$* mice, even when given a regular diet, displayed a higher tumor burden, reflected by increased numbers and sizes of tumors, again supporting the protective effect of

(A) Significant weight loss was documented in the control group compared with the three treatments ($n \geq 25$ in each group, experiments were repeated at least three times).
(B) Endoscopic evaluation shows a significant improvement in colitis score on day 12 for all 3 treatments. In comparison with arginine, citrulline was more beneficial ($n \geq 25$ in each group). Bottom: a representative image of the colon taken by colonoscopy.
(C) A representative plot showing a significant reduction in colon length in the control group compared with the treated colons ($n \geq 15$ in each group).
(D) The histological score for colitis was significantly lower in the treated colons compared with controls.
(E) Immunohistochemistry staining of colons for ASL shows higher expression after citrulline treatment compared with other treatments.
(F) FACS analysis showing that citrulline treatment is more effective than arginine in inducing NO synthesis in enterocytes.
(G) Terminal deoxynucleotidyl transferase dUTP nick end labeling (TUNEL) staining showing increased apoptosis in control colons compared with colons taken from mice treated with citrulline. Bottom: a quantification graph generated using Image-Pro Pulse software.
Error bars represent SEM.

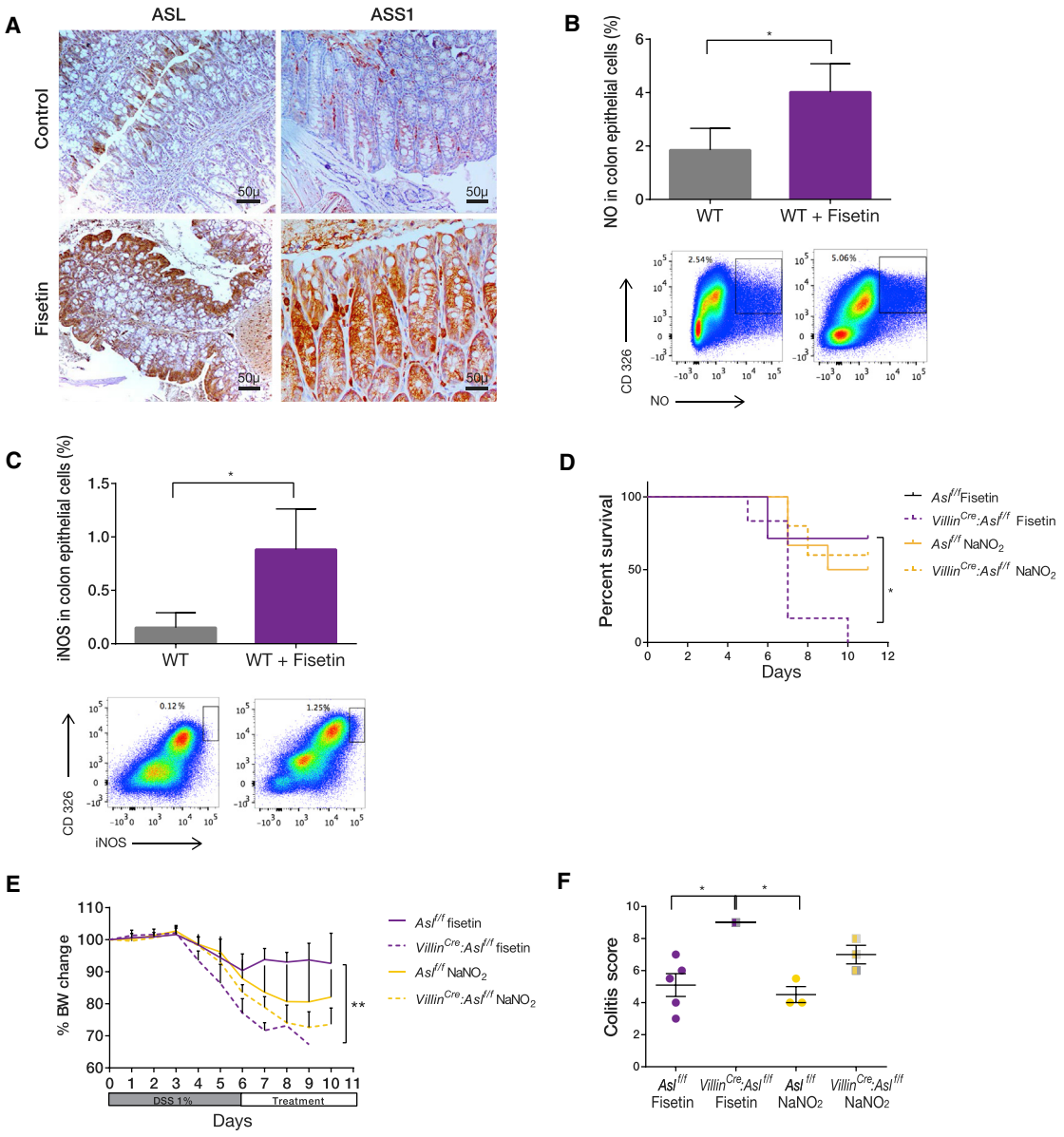

Figure 6. Induction of Endogenous NO Production by Enterocytes Alleviates Colitis

(A) Immunohistochemistry staining of distal colon sections after colitis induction shows up-regulation of ASL and ASS1 expression following fisetin treatment.

(B and C) FACS analysis of colon cells from mice treated with fisetin after colitis induction shows a significant increase in NO levels (B) and in iNOS expression (C) compared with cells from untreated controls.

(D–F) Colitis was induced in enterocyte CKO mice and littermate $Cre^{-/-}$ controls. Mice were treated with DSS for 5 days, followed by administration of either NO donors ($NaNO_2$) or fisetin ($n \geq 6$ in each group). Although NO donors were beneficial to both groups, fisetin treatment was not effective in *Villin*^{Cre}: *Asl*$^{f/f}$ mice, as shown by (D) decreased survival, (E) decreased body weight gain, and (F) a higher colitis score compared with controls.

Error bars represent SEM.

ASL upregulation in chronic inflammation (Figures 8A and 8B). Importantly, treatment of WT mice following the AOM-DSS protocol with our combined citrulline/fisetin treatment reduced colon cancer severity in all parameters evaluated (Figures 8C and 8D).

Collectively, our results show that NO levels can be metabolically modulated specifically in enterocytes by regulation of ASL function, which increases endogenous NO production at the precise amount and dosages needed to strengthen the epithelial barrier and, hence, mitigate colitis and decrease inflammation-associated colon cancer (Figure 8E).

DISCUSSION

IBD causes significant disease burden on affected individuals and their families and on the health care system (Limsrivilai

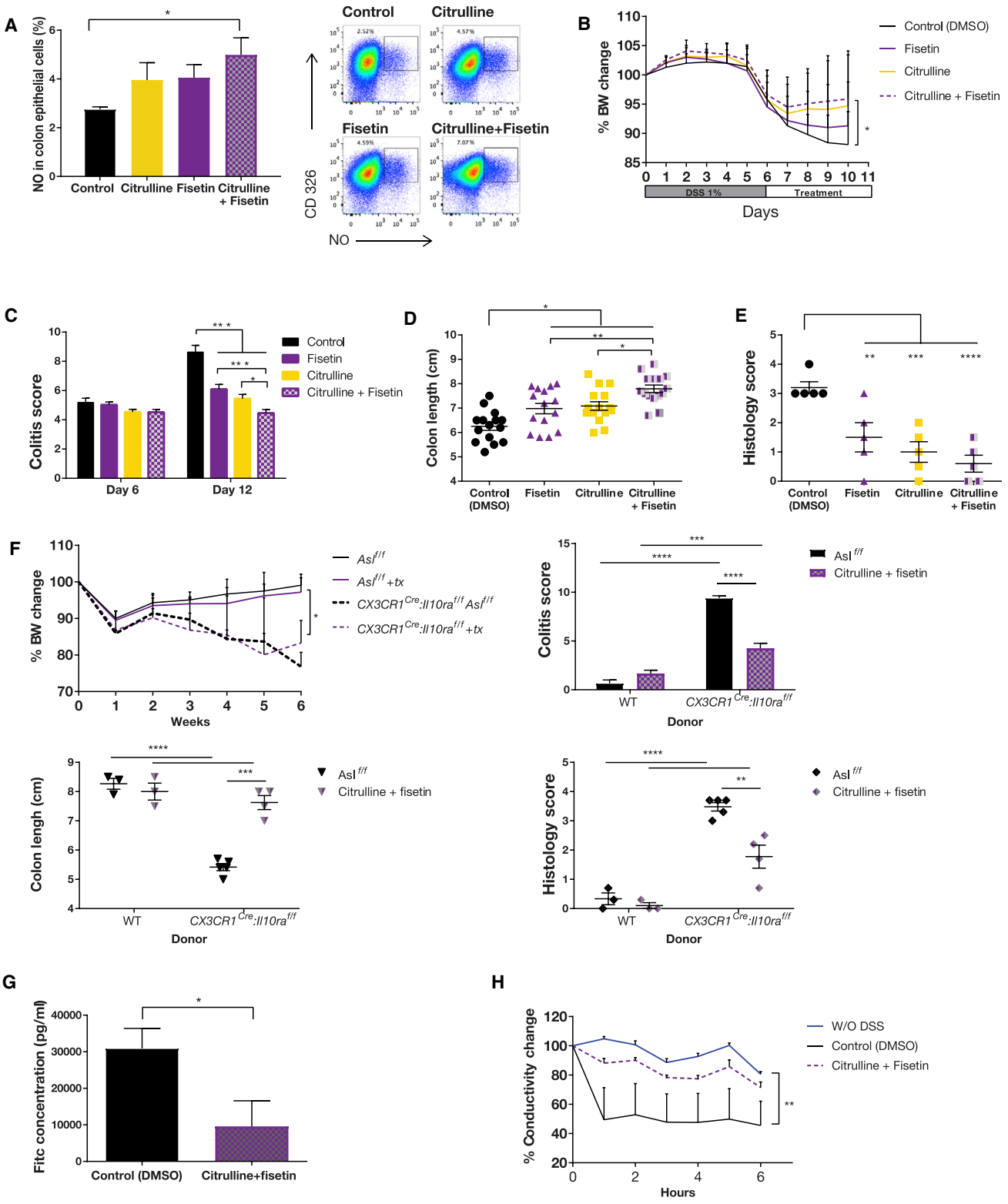

Figure 7. Enterocyte Self-Regulation of NO Levels Is the Most Beneficial Treatment for Colitis

Colitis was induced in C57BL/6J.OlaHsd mice with DSS for 6 days, followed by administration of either intraperitoneal (i.p.) fisetin, citrulline solution in drinking water, a combination of both treatments, or only DMSO as a control; the experiment was repeated 3 times.

(legend continued on next page)

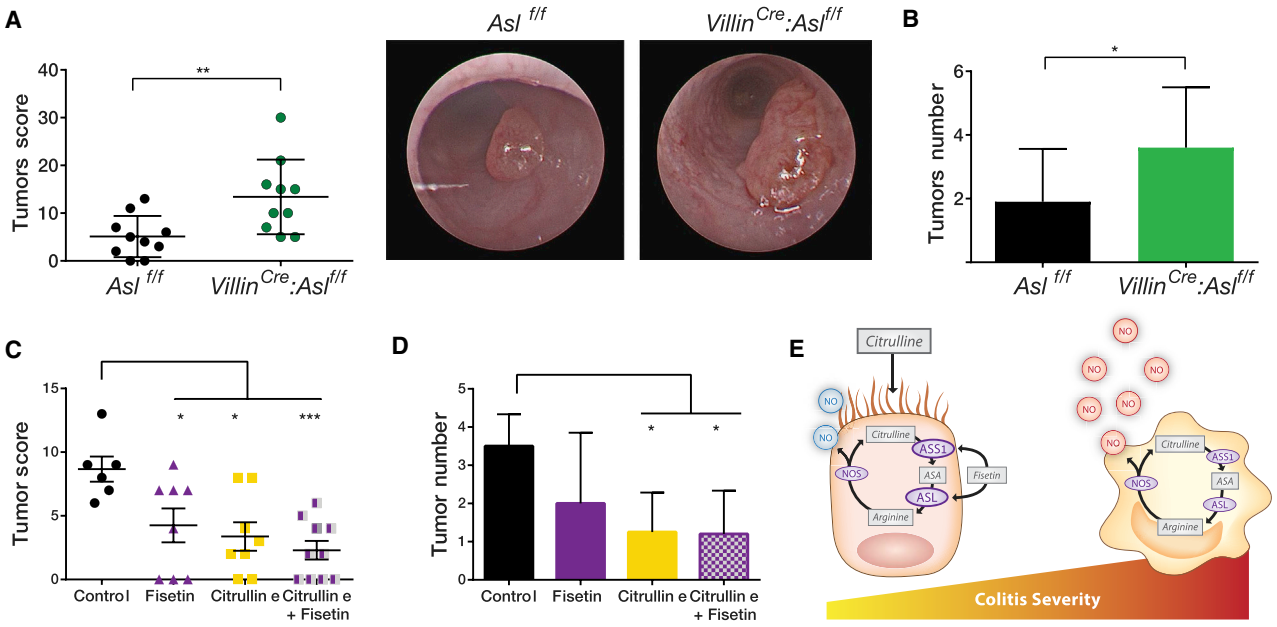

Figure 8. Metabolic Treatment Decreases Colitis Severity and Inflammation-Associated Colon Cancer

(A and B) The inflammation-associated cancer model was generated twice using the AOM-DSS model.

(A) A significant elevation in tumor score was seen in the *Villin^{Cre}:Asl$^{f/f}$* group compared with the control. Right: a representative image of the colon taken by colonoscopy.

(B) A significant increase in tumor number was seen in the *Villin^{Cre}:Asl$^{f/f}$* group compared with control mice.

(C and D) C57BL/6J.OlaHsd mice were treated with the AOM-DSS protocol. In addition, mice were treated for 15 days with either fisetin i.p., citrulline in drinking water, a combination of both treatments, or DMSO as a control. A significant elevation in tumor score (C) and tumor number (D) was seen in the treated groups compared with the control. The combined treatment was more beneficial compared with each treatment by itself ($n \geq 6$ in each group).

(E) A summary illustration demonstrating the distinct role of NO in each cell type. Although NO produced by macrophages is harmful, NO generated by enterocytes is protective. Colitis severity is reduced maximally by metabolically activating ASL in enterocytes using citrulline and fisetin supplementation.

Error bars represent SEM.

et al., 2017). Treatment is typically long-term or requires surgery, and, hence, adjuvant therapy that specifically targets key pathogenic mechanisms would be of significant value. NO has been known to play important but ambivalent roles in IBD (Cross and Wilson, 2003; Kolios et al., 2004). Indeed, in different models of colitis, inhibition of NO increased tissue injury, whereas, in other models, inhibition of NO provided benefits (Kolios et al., 2004). Similarly, administration of NOS inhibitors in general and of iNOS specifically for colitis treatment gave inconsistent results (Kubes, 2000; Miller et al., 1993, 1994). To add to this complexity, NO has been shown to play different roles along the colitis course, both in the inflammatory phase (Oshima et al., 2001) as well as in the regenerative phase (Aoi et al., 2008). These paradoxical and opposing results

(A) FACS analysis of colon epithelial cells from mice treated with the combined treatment shows a significant increase in NO levels compared with the control group (n = 4 in each group).

(B) A significant weight loss is documented in the control group compared with the treated mice ($n \geq 20$ in each group).

(C) An endoscopic evaluation demonstrates a significant improvement on day 12 in the colitis score of the treated groups compared with the control. Among the treatments, the combined treatment was the most beneficial ($n \geq 20$ in each group).

(D) A significant longer colon length is seen in the treated groups compared with the control. In addition, the colon is significantly longer with combined treatment compared with each treatment separately (n = 15 in both groups).

(E) A significant reduction in histological score in all treatment groups compared with the control.

(F and G) Colitis was induced by bone marrow (BM) implantation from either WT or *CX$_3$CR1^{Cre}:Il10ra $^{fl/fl}$* donors to lethally irradiated *Asl$^{f/f}$* mice. Two weeks after transplantation, mice were treated with a combination of citrulline and fisetin and compared with control animals treated with DMSO only. Colitis severity was evaluated 6 weeks after the implantation.

(F) No colitis signs were observed in animals implanted with WT donor BM. In animals implanted with *CX$_3$CR1^{Cre}:Il10ra $^{fl/fl}$* BM, a significant reduction in colitis severity was seen in treated animals compared with control mice, as shown by reduced weight loss (top left), a reduced colitis score (top right), increased colon length (bottom left), and a reduced histology score (bottom right) ($n > 5$ in each group, experiments were repeated twice).

(G) *In vivo* intestinal permeability assay to assess epithelial barrier function, performed using FITC-labeled dextran, showing significantly decreased permeability in treated mice compared with controls.

(H) Caco-2 cells plotted for resistance percentage over time, showing a significant decrease in conductivity of the control group compared with the group treated with citrulline and fisetin (the experiment included at least 5 biological repetitions).

Error bars represent SEM.

prevent implementation of NO-related drugs as a treatment regimen for colitis, and it is clear that there is a need to dissect the cell-specific contributions of NO in causation of IBD (Soliman and Mazzio, 1998). Because ASL is essential for NO production by all NOSs (Erez et al., 2011b), we abolished its expression in a cell-specific manner and defined a distinctive role for NO in each cell type.

Although the role of NO in promoting the immune response during colitis has been well established (Kolios et al., 2004), recent studies using different animal models propose that intestinal epithelial cells upregulate iNOS and NO levels against invading virulent pathogens as a host defense mechanism against intestinal infections (Meyerhoff et al., 2012; Vareille et al., 2008). Indeed, we find that promoting NO synthesis by elevating ASL expression with fisetin and citrulline was beneficial against colitis because it strengthened the epithelial barrier and prevented immune cell infiltration.

Emerging metabolic strategies have shown promise as treatments for inflammation and cancer by reducing the availability of glucose and glutamine levels, whereas therapies that increase inflammation and energy metabolites in the cancer microenvironment have been demonstrated to enhance tumor progression (Seyfried et al., 2015). We show here that boosting the metabolic ability of the enterocytes to synthesize and adjust the level and localization of NO to the exact amount and place where it is needed is the most beneficial treatment for reducing colitis severity. Because the duration, severity, and extent of colitis have all been shown to increase the risk for colon cancer development (Dyson and Rutter, 2012), not surprisingly, our combination of citrulline/fisetin also decreased inflammation-associated colon cancer.

Broadly, our study serves as a proof of concept for three main ideas. First, it confirms that regulating ASL allows metabolic regulation of NO in a cell-specific manner. Second, it shows that, during disease, cell-autonomous production of NO by iNOS can be protective as part of the intestinal innate immune response. Last, our study demonstrates the superior metabolic advantage of supplementing with substrates and upregulating the relevant metabolic enzymes over giving the deficient molecule directly as therapy. Because both citrulline and fisetin are nutraceutical agents that are available as supplements, the findings from this study could be translated rather straightforward into the human context.

EXPERIMENTAL PROCEDURES

Animals

Mice were monitored daily by staff and veterinary personnel for health and activity. Mice were given *ad libitum* access to water and standard mouse chow with 12-hr light/dark cycles. Colonies were maintained in a specific pathogen-free (SPF) barrier facility, with quarterly testing of pathogens in sentinel animals housed in the same room. All laboratory staff wore personal protective clothing, and all manipulations were performed in biosafety cabinets in procedure rooms in the same animal suite. All animal procedures were approved by the Institutional Animal Care and Use Committee (applications 07291113-2, 08020114-2, 24330116-3, 15990115-1, and 24340116-2) and performed in strict adherence to Weizmann Institute Animal Care and Use guidelines, following the NIH, European Commission, and Israeli guidelines. Mice were purchased from Jackson Laboratory (Bar Harbor, ME, USA). B6.Cg-Tg(Vav1-icre)A2Kio/J and B6.SJL-Tg(Vil-cre0997 Gum/J. C57BL/6JOlaHsd mice were purchased from ENVIGO RMS (ISRAEL). The B6.Cg-Tg (Itgax-cre)1-1Reiz/J. Cre mice were received from Prof. Jung.

Colitis induction experiments were conducted on 8- to 10-week-old male mice. Colitis-associated cancer experiments were conducted on 10- to 12-week-old female mice. Histologic sections of pups were taken from 10-day-old pups. Generation of BM chimeric mice was conducted on 10- to 12-week-old male mice.

Statistics

All statistical analyses were performed using one-way ANOVA, two-way ANOVA, repeated measures ANOVA, or Student's t test. Contrasts comparing groups with one specific treatment or control were tested with Dunnett's test. Log-transformed data were used where differences in variance were significant, and variances were correlated with means. Sample sizes were chosen in advance on the basis of common practice of the described experiment and are mentioned for each experiment. No statistical methods were used to predetermine sample size. Each experiment was conducted with biological and technical replicates and with three replications of the entire experiment unless specified otherwise. Statistical tests were done using Statsoft's STATISTICA, version 10. All error bars represent SE. $p < 0.05$ was considered significant in all analyses (*$p < 0.05$, **$p < 0.005$, ***$p < 0.0005$). A survival analysis, accounting for genotype and batch, was conducted using a Cox proportional hazards model (using the "survival" package in R).

SUPPLEMENTAL INFORMATION

Supplemental Information includes Supplemental Experimental Procedures, five figures, and one table and can be found with this article online at https://doi.org/10.1016/j.celrep.2018.04.053.

ACKNOWLEDGMENTS

We acknowledge and thank the Weizmann Institute for providing financial and infrastructural support. We are very thankful for the intellectual input of Prof. Brendan Lee and Prof. Eran Elinav. We appreciate the support given by Prof. Shimon Harrus, the statistical analysis by R. Rotkopf, and the technical contributions of Yuval Moshe, Yulia Frug, Amir Marinov, Sivan Galai, Jung-Seok Kim, and Sivan Pinto. A.E. is the incumbent of the Leah Omenn Career Development Chair and is supported by research grants from the European Research Program (CIG618113 and ERC614204), the Israel Science Foundation (1343/13 and 1952/13), and a Minerva grant award (711730). A.E. received additional support from the Adelis Foundation, the Henry S. and Anne S. Reich Research Fund, the Dukler Fund for Cancer Research, the Paul Sparr Foundation, the Saul and Theresa Esman Foundation, Joseph Piko Baruch, and the estate of Fannie Sherr. A. Sarver was supported by the Israel Cancer Research Fund (ICRF 711982). N.B.-P was supported by the European Research Council (IEMTx), D.d.B. and N.B.-P. was supported by Fondazione Telethon, and S.C.S.N. was supported by Baylor College of Medicine Intellectual and Developmental Disabilities Research Center Grant 1 U54 HD083092 and by the Doris Duke Charitable Foundation (DDCF 2013095).

AUTHOR CONTRIBUTIONS

N.S. conducted and was in charge of all experiments. C.R. and S.G.-C. conducted the FACS analysis. B.B. helped to generate the IL-10R-deficient colitis model. A. Sarver helped with NO analysis. J.F. preformed ELISA and cell culture experiments. A. Silberman and A.B. helped with the metabolic analysis. N.N.C.-N. analyzed human data. R.E. performed immunohistochemistry staining. I.B. performed MRI. M.P.-F. and N.Z. preformed 16S rRNA analysis. K.B.H. and S.I. performed the FISH experiments. R.M. and G.D. helped with the colonoscopy. N.N.C.-N. performed protein assays. D.d.B. and N.B.-P. performed the computational drug analysis. M.H.P. and S.C.S.N. gave scientific input. A.H. performed all pathological analyses and gave scientific input. S.J. helped design the studies and with writing the manuscript. A.E. was the leading scientist who initiated the study and wrote the manuscript.

DECLARATION OF INTERESTS

The authors declare no competing interests.

Received: November 26, 2017
Revised: February 5, 2018
Accepted: April 12, 2018
Published: May 15, 2018

REFERENCES

Alican, I., and Kubes, P. (1996). A critical role for nitric oxide in intestinal barrier function and dysfunction. Am. J. Physiol. *270*, G225–G237.

Aoi, Y., Terashima, S., Ogura, M., Nishio, H., Kato, S., and Takeuchi, K. (2008). Roles of nitric oxide (NO) and NO synthases in healing of dextran sulfate sodium-induced rat colitis. J. Physiol. Pharmacol *59*, 315–336.

Araki, Y., Sugihara, H., and Hattori, T. (2006). In vitro effects of dextran sulfate sodium on a Caco-2 cell line and plausible mechanisms for dextran sulfate sodium-induced colitis. Oncol. Rep. *16*, 1357–1362.

Atreya, R., and Neurath, M.F. (2015). IBD pathogenesis in 2014: Molecular pathways controlling barrier function in IBD. Nat. Rev. Gastroenterol. Hepatol. *12*, 67–68.

Barral, M., Dohan, A., Allez, M., Boudiaf, M., Camus, M., Laurent, V., Hoeffel, C., and Soyer, P. (2016). Gastrointestinal cancers in inflammatory bowel disease: An update with emphasis on imaging findings. Crit. Rev. Oncol. Hematol. *97*, 30–46.

Blaise, G.A., Gauvin, D., Gangal, M., and Authier, S. (2005). Nitric oxide, cell signaling and cell death. Toxicology *208*, 177–192.

Boughton-Smith, N.K., Evans, S.M., Hawkey, C.J., Cole, A.T., Balsitis, M., Whittle, B.J., and Moncada, S. (1993). Nitric oxide synthase activity in ulcerative colitis and Crohn's disease. Lancet *342*, 338–340.

Brown, J.F., Keates, A.C., Hanson, P.J., and Whittle, B.J. (1993). Nitric oxide generators and cGMP stimulate mucus secretion by rat gastric mucosal cells. Am. J. Physiol. *265*, G418–G422.

Bustos, R., and Sobrino, F. (1992). Stimulation of glycolysis as an activation signal in rat peritoneal macrophages. Effect of glucocorticoids on this process. Biochem. J. *282*, 299–303.

Caton, M.L., Smith-Raska, M.R., and Reizis, B. (2007). Notch-RBP-J signaling controls the homeostasis of CD8- dendritic cells in the spleen. J. Exp. Med. *204*, 1653–1664.

Coëffier, M., Marion-Letellier, R., and Déchelotte, P. (2010). Potential for amino acids supplementation during inflammatory bowel diseases. Inflamm. Bowel Dis. *16*, 518–524.

Cooper, H.S., Murthy, S.N., Shah, R.S., and Sedergran, D.J. (1993). Clinicopathologic study of dextran sulfate sodium experimental murine colitis. Lab. Invest. *69*, 238–249.

Cortese-Krott, M.M., and Kelm, M. (2014). Endothelial nitric oxide synthase in red blood cells: key to a new erythrocrine function? Redox Biol. *2*, 251–258.

Cross, R.K., and Wilson, K.T. (2003). Nitric oxide in inflammatory bowel disease. Inflamm. Bowel Dis. *9*, 179–189.

De Jonge, W.J., Dingemanse, M.A., de Boer, P.A.J., Lamers, W.H., and Moorman, A.F.M. (1998). Arginine-metabolizing enzymes in the developing rat small intestine. Pediatr. Res. *43*, 442–451.

de Souza, H.S.P., and Fiocchi, C. (2016). Immunopathogenesis of IBD: current state of the art. Nat. Rev. Gastroenterol. Hepatol. *13*, 13–27.

Dyson, J.K., and Rutter, M.D. (2012). Colorectal cancer in inflammatory bowel disease: what is the real magnitude of the risk? World J. Gastroenterol. *18*, 3839–3848.

Eiserich, J.P., Hristova, M., Cross, C.E., Jones, A.D., Freeman, B.A., Halliwell, B., and van der Vliet, A. (1998). Formation of nitric oxide-derived inflammatory oxidants by myeloperoxidase in neutrophils. Nature *391*, 393–397.

Erez, A., Nagamani, S.C., and Lee, B. (2011a). Argininosuccinate lyase deficiency-argininosuccinic aciduria and beyond. Am. J. Med. Genet. C. Semin. Med. Genet. *157C*, 45–53.

Erez, A., Nagamani, S.C.S., Shchelochkov, O.A., Premkumar, M.H., Campeau, P.M., Chen, Y., Garg, H.K., Li, L., Mian, A., Bertin, T.K., et al. (2011b). Requirement of argininosuccinate lyase for systemic nitric oxide production. Nat. Med. *17*, 1619–1626.

Glocker, E.-O., Kotlarz, D., Boztug, K., Gertz, E.M., Schäffer, A.A., Noyan, F., Perro, M., Diestelhorst, J., Allroth, A., Murugan, D., et al. (2009). Inflammatory bowel disease and mutations affecting the interleukin-10 receptor. N. Engl. J. Med. *361*, 2033–2045.

Guzik, T.J., Korbut, R., and Adamek-Guzik, T. (2003). Nitric oxide and superoxide in inflammation and immune regulation. J. Physiol. Pharmacol *54*, 469–487.

Iorio, F., Bosotti, R., Scacheri, E., Belcastro, V., Mithbaokar, P., Ferriero, R., Murino, L., Tagliaferri, R., Brunetti-Pierri, N., Isacchi, A., and di Bernardo, D. (2010). Discovery of drug mode of action and drug repositioning from transcriptional responses. Proc. Natl. Acad. Sci. USA *107*, 14621–14626.

Kelly, B., and O'Neill, L.A.J. (2015). Metabolic reprogramming in macrophages and dendritic cells in innate immunity. Cell Res. *25*, 771–784.

King, J.B., von Furstenberg, R.J., Smith, B.J., McNaughton, K.K., Galanko, J.A., and Henning, S.J. (2012). CD24 can be used to isolate Lgr5+ putative colonic epithelial stem cells in mice. Am. J. Physiol. Gastrointest. Liver Physiol. *303*, G443–G452.

Knowles, R.G., and Moncada, S. (1994). Nitric oxide synthases in mammals. Biochem. J. *298*, 249–258.

Kolios, G., Valatas, V., and Ward, S.G. (2004). Nitric oxide in inflammatory bowel disease: a universal messenger in an unsolved puzzle. Immunology *113*, 427–437.

Kubes, P. (2000). Inducible nitric oxide synthase: a little bit of good in all of us. Gut *47*, 6–9.

Limsrivilai, J., Stidham, R.W., Govani, S.M., Waljee, A.K., Huang, W., and Higgins, P.D.R. (2017). Factors that predict high health care utilization and costs for patients with inflammatory bowel diseases. Clin. Gastroenterol. Hepatol. *15*, 385–392.e2.

Lorsbach, R.B., Murphy, W.J., Lowenstein, C.J., Snyder, S.H., and Russell, S.W. (1993). Expression of the nitric oxide synthase gene in mouse macrophages activated for tumor cell killing. Molecular basis for the synergy between interferon-gamma and lipopolysaccharide. J. Biol. Chem. *268*, 1908–1913.

Madison, B.B., Dunbar, L., Qiao, X.T., Braunstein, K., Braunstein, E., and Gumucio, D.L. (2002). Cis elements of the villin gene control expression in restricted domains of the vertical (crypt) and horizontal (duodenum, cecum) axes of the intestine. J. Biol. Chem. *277*, 33275–33283.

Marini, J.C., Agarwal, U., and Didelija, I.C. (2015). Dietary arginine requirements for growth are dependent on the rate of citrulline production in mice. J. Nutr. *145*, 1227–1231.

Martin, D.R., Danrad, R., Herrmann, K., Semelka, R.C., and Hussain, S.M. (2005). Magnetic resonance imaging of the gastrointestinal tract. Top. Magn. Reson. Imaging *16*, 77–98.

Meyerhoff, R.R., Nighot, P.K., Ali, R.A., Blikslager, A.T., and Koci, M.D. (2012). Characterization of turkey inducible nitric oxide synthase and identification of its expression in the intestinal epithelium following astrovirus infection. Comp. Immunol. Microbiol. Infect. Dis. *35*, 63–69.

Mian, A.I., Aranke, M., and Bryan, N.S. (2013). Nitric oxide and its metabolites in the critical phase of illness: rapid biomarkers in the making. Open Biochem. J. *7*, 24–32.

Middleton, S.J., Shorthouse, M., and Hunter, J.O. (1993). Increased nitric oxide synthesis in ulcerative colitis. Lancet *341*, 465–466.

Miller, M.J., Chotinaruemol, S., Sadowska-Krowicka, H., Kakkis, J.L., Munshi, U.K., Zhang, X.J., and Clark, D.A. (1993). Nitric oxide: the Jekyll and Hyde of gut inflammation. Agents Actions *39*, C180–C182.

Miller, M.J., Munshi, U.K., Sadowska-Krowicka, H., Kakkis, J.L., Zhang, X.J., Eloby-Childress, S., and Clark, D.A. (1994). Inhibition of calcium-dependent

nitric oxide synthase causes ileitis and leukocytosis in guinea pigs. Dig. Dis. Sci. *39*, 1185–1192.

Moncada, S. (1992). The 1991 Ulf von Euler Lecture. The L-arginine: nitric oxide pathway. Acta Physiol. Scand. *145*, 201–227.

Nagamani, S.C., Erez, A., and Lee, B. (2012). Argininosuccinate lyase deficiency. Genet. Med. *14*, 501–507.

Ogilvy, S., Elefanty, A.G., Visvader, J., Bath, M.L., Harris, A.W., and Adams, J.M. (1998). Transcriptional regulation of vav, a gene expressed throughout the hematopoietic compartment. Blood *91*, 419–430.

Oshima, T., Jordan, P., Grisham, M.B., Alexander, J.S., Jennings, M., Sasaki, M., and Manas, K. (2001). TNF-alpha induced endothelial MAdCAM-1 expression is regulated by exogenous, not endogenous nitric oxide. BMC Gastroenterol. *1*, 5.

Pegg, A.E. (2016). Functions of Polyamines in Mammals. J. Biol. Chem. *291*, 14904–14912.

Premkumar, M.H., Sule, G., Nagamani, S.C., Chakkalakal, S., Nordin, A., Jain, M., Ruan, M.Z., Bertin, T., Dawson, B., Zhang, J., et al. (2014). Argininosuccinate lyase in enterocytes protects from development of necrotizing enterocolitis. Am. J. Physiol. Gastrointest. Liver Physiol. *307*, G347–G354.

Rath, M., Müller, I., Kropf, P., Closs, E.I., and Munder, M. (2014). Metabolism via Arginase or Nitric Oxide Synthase: Two Competing Arginine Pathways in Macrophages. Front. Immunol. *5*, 532.

Rosenberg, I., Cherayil, B.J., Isselbacher, K.J., and Pillai, S. (1991). Mac-2-binding glycoproteins. Putative ligands for a cytosolic beta-galactoside lectin. J. Biol. Chem. *266*, 18731–18736.

Sahu, B.D., Kumar, J.M., and Sistla, R. (2016). Fisetin, a dietary flavonoid, ameliorates experimental colitis in mice: Relevance of NF-κB signaling. J. Nutr. Biochem. *28*, 171–182.

Sambuy, Y., De Angelis, I., Ranaldi, G., Scarino, M.L., Stammati, A., and Zucco, F. (2005). The Caco-2 cell line as a model of the intestinal barrier: influence of cell and culture-related factors on Caco-2 cell functional characteristics. Cell Biol. Toxicol. *21*, 1–26.

Seyfried, T.N., Flores, R., Poff, A.M., D'Agostino, D.P., and Mukherjee, P. (2015). Metabolic therapy: a new paradigm for managing malignant brain cancer. Cancer Lett. *356* (*2 Pt A*), 289–300.

Shah, V., Lyford, G., Gores, G., and Farrugia, G. (2004). Nitric oxide in gastrointestinal health and disease. Gastroenterology *126*, 903–913.

Soliman, K.F.A., and Mazzio, E.A. (1998). In vitro attenuation of nitric oxide production in C6 astrocyte cell culture by various dietary compounds. Proc. Soc. Exp. Biol. Med. *218*, 390–397.

Soufli, I., Toumi, R., Rafa, H., and Touil-Boukoffa, C. (2016). Overview of cytokines and nitric oxide involvement in immuno-pathogenesis of inflammatory bowel diseases. World J. Gastrointest. Pharmacol. Ther. *7*, 353–360.

Suschek, C.V., Schnorr, O., and Kolb-Bachofen, V. (2004). The role of iNOS in chronic inflammatory processes in vivo: is it damage-promoting, protective, or active at all? Curr. Mol. Med. *4*, 763–775.

Thaker, A.I., Shaker, A., Rao, M.S., and Ciorba, M.A. (2012). Modeling colitis-associated cancer with azoxymethane (AOM) and dextran sulfate sodium (DSS). J. Vis. Exp. *67*, 4100.

Vander Lugt, B., Khan, A.A., Hackney, J.A., Agrawal, S., Lesch, J., Zhou, M., Lee, W.P., Park, S., Xu, M., DeVoss, J., et al. (2014). Transcriptional programming of dendritic cells for enhanced MHC class II antigen presentation. Nat. Immunol. *15*, 161–167.

Vareille, M., Rannou, F., Thélier, N., Glasser, A.L., de Sablet, T., Martin, C., and Gobert, A.P. (2008). Heme oxygenase-1 is a critical regulator of nitric oxide production in enterohemorrhagic Escherichia coli-infected human enterocytes. J. Immunol. *180*, 5720–5726.

Vatassery, G.T., SantaCruz, K.S., DeMaster, E.G., Quach, H.T., and Smith, W.E. (2004). Oxidative stress and inhibition of oxidative phosphorylation induced by peroxynitrite and nitrite in rat brain subcellular fractions. Neurochem. Int. *45*, 963–970.

Whittem, C.G., Williams, A.D., and Williams, C.S. (2010). Murine colitis modeling using dextran sulfate sodium (DSS). J. Vis. Exp *35*, 1652.

Wijnands, K.A.P., Vink, H., Briedé, J.J., van Faassen, E.E., Lamers, W.H., Buurman, W.A., and Poeze, M. (2012). Citrulline a more suitable substrate than arginine to restore NO production and the microcirculation during endotoxemia. PLoS ONE *7*, e37439.

Witthöft, T., Eckmann, L., Kim, J.M., and Kagnoff, M.F. (1998). Enteroinvasive bacteria directly activate expression of iNOS and NO production in human colon epithelial cells. Am. J. Physiol. *275*, G564–G571.

Zigmond, E., Bernshtein, B., Friedlander, G., Walker, C.R., Yona, S., Kim, K.-W., Brenner, O., Krauthgamer, R., Varol, C., Müller, W., and Jung, S. (2014). Macrophage-restricted interleukin-10 receptor deficiency, but not IL-10 deficiency, causes severe spontaneous colitis. Immunity *40*, 720–733.

Cell Reports, Volume *23*

Supplemental Information

Induction of Nitric-Oxide Metabolism in Enterocytes Alleviates Colitis and Inflammation-Associated Colon Cancer

Noa Stettner, Chava Rosen, Biana Bernshtein, Shiri Gur-Cohen, Julia Frug, Alon Silberman, Alona Sarver, Narin N. Carmel-Neiderman, Raya Eilam, Inbal Biton, Meirav Pevsner-Fischer, Niv Zmora, Alexander Brandis, Keren Bahar Halpern, Ram Mazkereth, Diego di Bernardo, Nicola Brunetti-Pierri, Muralidhar H. Premkumar, Gillian Dank, Sandesh C.S. Nagamani, Steffen Jung, Alon Harmelin, and Ayelet Erez

Supplementary Experimental Procedures

Colitis induction: Colitis was induced in *Vav1^{Cre}:Asl$^{f/f}$* mice and *CD11c^{Cre}:Asl$^{f/f}$* mice with 1.5% DSS and with 0.8% DSS in the *Villin^{Cre}:Asl$^{f/f}$* (wt/vol), (Dextran Sodium Sulfate, MP Biomedicals; molecular weight 36,000–50,000 Da). The powder was dissolved in the drinking water for 6 days, followed by 5 days of supplementing regular water (Wirtz et al., 2007). Each group consisted of eight to ten, 8-10 weeks old, male mice. Experiments were repeated at least three times.

Generation of BM chimeric mice. *Villin^{Cre}:Asl$^{f/f}$* or Asl$^{f/f}$ male mice aged 10–12 weeks were used as recipients. Mice were irradiated with a dose of 950 Gy and reconstituted via IV injection with 5×10^6 BM cells of either wt or *CX$_3$CR1^{Cre}:Il10ra $^{fl/fl}$* mice.

Arginine free diet: mice received arginine free diet (Envigo,TD09152 TEKLAD) since weaning and along the experiment.

Endoscopic evaluation of colitis: Colonoscopy was performed on days 7 and 11 of the experiment to monitor for severity of colitis. For the procedure, a high resolution mouse video endoscopic system was used, which consists of a miniature endoscope (scope 1.9 mm outer diameter), a xenon light source, a triple chip camera, and an air pump to achieve regulated inflation of the mouse bowel (Karl Storz, Tuttlingen, Germany). Mice were anesthetized by the administration of 100 mg/kg Ketamine/10 mg/kg Xylazine mixture IP, after which, the endoscope was introduced via the anus and the colon was carefully insufflated with an air pump before analysis of the colonic mucosa. The endoscopic procedure was viewed on a color monitor and digitally recorded on tape. Colitis was scored according to the Murine endoscopic index of colitis severity (MEICS), considering differences in the thickness of the bowel wall, changes in blood vessel integrity, mucosal surface, stool consistency or the presence of fibrin, scored each between 0 and 3. The cumulative score ranged from 0 (no signs of inflammation) to 15 (signs of severe inflammation) (Becker et al., 2006).

Drug administration: Mice were treated with 1% (wt/vol) DSS for 6 days, followed by administration of either arginine (Sigma-Aldrich, St. Louis, MO, catalogue number A8094) 1% (wt/vol) solution in drinking water, citrulline 1% (wt/vol) (L-citrulline, Chem-Impex International), $NaNO_2$ 100mg/kg (Sigma-Aldrich, St. Louis, MO, catalogue number S2252), or water as control for additional 6 days.

Fisetin was given by i.p. injection (1 mg/animal) in 30 µL of DMSO twice weekly. The control group was injected with 30 µL of DMSO twice weekly. Each group consisted of ten, 8 weeks old, male mice. Experiments were repeated three times.

Colitis associated cancer induction: 10- to 12 weeks old female mice, each group consisted of eight to ten mice, were injected with Azoxymethane (AOM) (Sigma) intraperitoneally at a dose of 12.5 mg/kg body weight. After 6 d, *Villin^{Cre}:Asl$^{f/f}$* mice were treated with 2% DSS (MP Biomedicals) (M.W. 36,000–50,000 Da) in the drinking water for 5 d, then followed by 16 d of regular water. This cycle was repeated twice. C57BL/6J.OlaHsd mice were treated with 1.5% DSS in the drinking water for 6 days followed by 15 d of administration of either fisetin (1mg in 30µl DMSO IP, twice, in 7 days interval) citrulline 1% (wt/vol) solution in drinking water, the combination of both treatments or only DMSO as a control (30µl DMSO IP, twice, in 7 days interval). This cycle was repeated twice. Colonoscopy was performed on days 40, 60 and 80 of the experiment. Tumorigenesis was evaluated according to previously described tumor scoring system (Becker et al., 2006).

Histopathology. On the day of sacrifice, colons were removed and their length was measured. Colon was fixed in 2.5% PFA solution overnight at 4°C, then embedded in paraffin, sectioned and stained with H&E. Tissues were examined in a blinded manner by a pathologist and scored on a 0–4 scale based on the parameters of inflammation severity(Hs et al., 1993). Histologic evaluation of *CX$_3$CR1^{Cre}:Il10ra $^{fl/fl}$* mice as previously described (Zigmond et al., 2014). Briefly, three segments of the colon (proximal colon, medial colon and distal colon-rectum) were given a score between 0-4 and the summation of these scores provided a total colonic disease score.

Immunohistochemistry: Four micrometer paraffin embedded tissue sections were deparaffinized and rehydrated. Endogenous peroxidase was blocked with three percent H2O2 in methanol. Sections undergoing for ALS staining were incubated in cold acetone at -20ºc for 7 minutes. For F4/80 and MAC-2 staining, we performed antigen retrieval in Tris-EDTA pH9 and 10 mM citric acid pH 6, for 10 min respectively, using a low boiling program in the microwave to break protein cross-links and unmask antigens. After pre-incubation with 20% normal horse serum and 0.2% Triton X-100 for 1 hour at RT, sections were incubated with the primary antibodies as follow; ASL (1:100, Abcam, ab97370, CA, USA); F4/80 (1:50, Serotec, Kidllington, UK); Mac-2 (1:400, Cedarlane, NC, USA); for fluorescent double-staining of ASL and CD11c we used mouse anti ASL (1:50 Santa Cruz

Biotechnology, Inc. sc-166787, TX, USA) and rabbit anti CD11c (1:50, ab52632) . All antibodies were diluted in PBS containing 2% normal horse serum and 0.2% Triton. Sections were incubated overnight at RT followed by 48h at 4°C. Sections were washed three times in PBS and incubated with secondary biotinylated IgG at RT for 1.5 hour, washed three times in PBS and incubated with avidin-biotin Complex (*elite* ABC kit, Vector Lab, CA, USA) at RT for additional 90 min followed by DAB (Sigma) reaction. For the fluorescent staining we used CY2 conjugated anti mouse and CY3 conjugated streptavidin (1:100 and 1;200 respectively, Jackson ImmunoResearch, West Grove, PA)
Tunnel staining was performed by using ApopTag kit detection according to manufacturer's instructions (Millipore, CA, USA). Stained sections were examined and photographed by a fluorescence or bright field microscope (Eclipse Ni-U; Nikon, Tokyo, Japan) equipped with Plan Fluor objectives (10; 20x; 40x) connected to a monochrome camera (DS-Qi1, Nikon).

***In vivo* intestinal permeability assay.** To assess barrier function was performed using an FITC-labeled dextran method. Food and water were withdrawn for 3h and mice were orally administrated with permeability tracer (80 mg/100 g body weight of FITC-labeled dextran, MW 4000; FD4, Sigma-Aldrich). Serum was collected retro-orbitally three hours later and fluorescence intensity was determined (excitation, 492 nm; emission, 525 nm; BioTek). FITC-dextran concentrations were determined using a standard curve generated by serial dilution of FITC-dextran.

Nitrite and nitrate concentrations in blood, colon: On the day of sacrifice, blood and 1cm of the distal colon were collected. Blood was separated by centrifuge (1500 RPM for 5 minutes) to plasma and red blood cells (RBC). Colon tissue was homogenized. Proteins in each sample were removed by centrifugation at 10,000g for 5 min following methanol precipitation (colon:methanol = 1:2 weight/volume, RBC:methanol = 1:1 volume/volume, 4 ^{o}C).
Nitrite concentration in the colon and the plasma was measured using a dedicated HPLC system (ENO-20; EiCom, Kyoto, Japan). This method is based on the separation of nitrite and nitrate by ion chromatography, followed by on-line reduction of nitrate to nitrite, post column derivatization with Griess reagent, and detection at 540 nm. Proteins in each sample were removed by centrifugation at 10,000g for 5 min following methanol precipitation (colon:methanol = 1:2 weight/volume, plasma:methanol = 1:1 volume/volume, 4°C).

Mouse colon epithelial and lamina propria isolation: To achieve cell purity, we used the 2 step protocol for isolation of different intestinal compartments (Berger et al., 2017; Elinav et al.,

2011); first we isolated intestinal epithelium and then, we isolated lamina propria CD45+ cells. The purity of different compartments was quality tested by staining for CD326 and CD45 markers respectively (King et al., 2012). Colon segment was flushed with cold PBS, longitudinally cut open and rinsed to remove residual luminal contents. Tissue was cut into 3- to 5-mm pieces and incubated in HBSS medium containing EDTA 0.5M and Hepes10mM at 37°C for 20 min, shaken at 180 rpm, to separate epithelial fraction. Supernatant was centrifuged at 4°C at 500 g for 10 minutes. Recovered tissue was digested in HBSS medium with 2% fetal bovine serum (FBS), 0.05% collagenase II and 0.05% DNase I (Sigma) for 40 min. at 37°C, shaken at 180 rpm. LP cells were filtered through 65μm mesh and centrifuged at 4°C at 500 g for 10 minutes.

Flow cytometry: We prepared single cell suspensions from mouse colon by enzymatic digestion and analyzed by polychromatic flow cytometry. Samples were stained with conjugated antibodies or matching isotype controls according to manufacturer's instructions. Data were acquired on an LSRII (BD Biosciences) or FACSCalibur instrument (Becton-Dickinson) with CellQuest software, with a MacsQuant instrument (Miltenyi, Bergisch Gladbach, Germany), and analyzed using BD FACSDiva 6 or FlowJo software (version 7.6.5, or version vX.0.7 Tree Star Inc) or MacsQuant. Colon cells were stained for 30 min at 4 °C in flow cytometry buffer (PBS, 10% FCS and 0.02% azide). For antigens that require intracellular staining (Asl, iNOS and S-nitrosocystein), cell surface staining was followed by cell fixation and permeabilization with the Cytofix/Cytoperm kit (BD Biosciences) according to the manufacturer's instructions. For staining, we used a lineage cocktail of antibodies anti-CD45-APC, Anti-CD64-PE, Anti – CD11c-PB, Anti-326-APC cy7, Anti CD31-PE cy7 (all from BioLegend). After staining for cell surface antigens, intracellular NO was detected by incubation of cells for 15 min at 37 °C with 10 μM DAF-FM diacetate followed by extensive washing, according to the manufacturer's instructions (Molecular Probes). Staining without addition of the DAF-FM probe was considered to be the baseline for gating the positive population. Asl was detected using anti-Asl- ALEXA FLUOR® 488 (BD Biosciences), iNOS using anti-iNOS followed by anti-rat 488 (Jackson ImmunoResearch), and nitrosylation using anti-S-nitrosocystein (from abcam) followed by anti-mouse 488 (Jackson ImmunoResearch).

Macrophage elicitation and stimulation: Thioglycollate elicited macrophages were isolated by peritoneal lavage from five, 8 weeks old mice, in each group. Mice were i.p. injected with 1ml sterile thioglycollate broth and four days after, peritoneal macrophages were isolated following a previously described method by Zhang et al. (Zhang et al., 2008).

Equal numbers of peritoneal cells were allowed to adhere to cell culture dishes, two plates for each extract, for four hours. Non-adhered cells were removed and adherent cells were washed twice. Cells were cultured in RPMI 1640 arginine free medium containing 20% fetal calf serum (heat inactivated), 1% Penicillin/Streptomycin and 2% L-Glutamine (all from Biological Industries). For each extract, one plate was stimulated with LPS ultrapure (1µg/ml) (Lipopolysaccharide, Ultra Pure, Salmonella, Sigma-Aldrich), for a total of 18h or 36 h while the other plate served as control. Medium was taken for NO analysis and glucose and lactate levels using NOVA.

Assessment of plasma arginine concentrations: Blood was collected at the time of sacrifice via cardiac puncture, placed in heparin coated tube and kept on ice. The samples were centrifuged for 5 min at 7,000 rpm. The supernatant was removed, aliquoted, snap frozen, and stored at -80°C until used for amino acid analysis. Analysis was conducted by analytical laboratory services (AMINOLAB LTD).

Assessment of colon epithelial cells arginine and polyamines concentrations: The analysis was performed according to a previously described protocol (Gray and Plumb, 2014) with slight modifications. Briefly, equal number of isolated colon epithelial cells (~$3*10^6$) were incubated in a phosphoric:acetic acid buffer supplemented with 1:50 (v/v; 10 µM) of the following internal standards: hexamethylene diamine and 13C6-arginine (Cambridge Isotope Laboratories). Following 30 min at 40C, cell lysates went through three freeze-thaw cycles using liquid nitrogen.

For the determination of polyamines and amino acids, equal protein 10-µl samples (12 µg) were added to 70 µL of borate buffer (200 mM, pH 8.8 at 25°C) and mixed. Then, 20 µl of Aqc reagent (10 mM dissolved in 100% ACN) were added and immediately mixed. Aqc reagent was prepared following the procedure described (Cohen and Michaud, 1993). For the determination of proline and arginine, samples were first diluted with the borate buffer 1:10, and then 10-µl aliquots were reacted with Aqc. For derivatization, the samples were heated at 55°C for 10

minutes, centrifuged at maximum speed for three min and then filtered through a 0.2-µm PTFE filter (Millex-LG, Millipore) to HPLC vials containing inserts.

The LC-MS/MS instrument consisted of Acquity I-class UPLC system and Xevo TQ-S triple quadrupole mass spectrometer (Waters). Chromatographic conditions were used as described in (Gray and Plumb, 2014). Mass detection was carried out using electrospray ionization in the positive mode. Argon was used as the collision gas with a flow of 0.1 ml/min. The capillary voltage was set to 3.0 kV, source temperature - 150°C, desolvation temperature - 650°C, desolvation gas flow - 800 L/min, cone voltage 20V. Analytics were detected by monitoring of fragment ion 171 m/z produced from corresponding precursor ions using parameters described in (Zwighaft et al., 2015) for polyamines, and in (Gray and Plumb, 2014) for amino acids, with exception that collision energy 20eV was used for regular and labeled 13C6 arginine.

The concentrations were calculated as the response ratio between IS and the analyte using calibration curves of the corresponding compounds. Data processing was performed with TargetLynx software.

ELISA: For cytokine production measurements, colon tissue single cell suspension was assayed for cytokine levels using a mouse cytokine quantibody array (RayBiotech), according to the manufacturer's instructions. Nitrosilation level was measured using 3-Nitrotyrosine ELISA Kit (abcam), according to the manufacturer's instructions.

Complete blood count: Blood was collected at the time of sacrifice via cardiac puncture, placed in EDTA coated tube. Diagnostic Veterinary Pathology Services (PathoVet).

DNA extraction from blood: QIAamp DNA Blood Mini Kit (Qiagen, Hilden, Germany) (Qiagen, Valencia, CA), DNA was isolated from 200 µl of blood according to manufacturer's instruction, in the final step DNA was eluted in 200 µL of buffer AE. The DNA eluate was stored at - 20°C until use in qPCR analysis.

Western blot: Western blotting was performed as previously described (Becker systems (Perkin Elmer) and a fluorescence microscope (Olympus, et al., 2003). In some experiments, culture supernatants were used and concentrated by acetone precipitation. Equal amounts of extract (30 or 50 µg) were added to 10 µl electrophoresis sample buffer. After boiling, the proteins were separated by 10% SDS - PAGE, then transferred to nitrocellulose membranes and detected with a specific antibody Anti-Argininosuccinate Lyase (ab97370) and the ECL Western blotting analysis system (Amersham).

Small molecule screen analysis: MANTRA (Iorio et al., 2010; Napolitano et al., 2016) is built upon the Connectivity Map dataset (Lamb et al., 2006) where 1,309 small molecules have been profiled by Affymetrix microarrays on 5 different cell lines at different dosages for a total of 7,000 gene expression profiles (GEPs). MANTRA collapses the 7,000 GEPs into 1,309 Prototype Ranked Lists (PRLs), i.e. one for each small molecule. PRLs represent a consensus rank of differentially expressed genes following treatment with the same drug across multiple cell lines and different dosages. In order to identify the drugs upregulating ASS1 and ASL, we performed a Gene Set Enrichment Analysis (GSEA) on the PRLs for each of 1,309 drugs using the MANTRA online web tool (http://mantra.tigem.it).

MRI: Prior to MRI imaging, animals were anesthetized using a mix of Medetomidine/Ketamine. The mouse colon was cleaned using warm water and perfluorinated oil was introduced into the colon via a rectal catheter. MRI experiments were performed on a 9.4T Bruker BioSpec system using a quadrature volume coil with 35-mm inner diameter. T2 maps were acquired using a multi-slice, spin-echo imaging sequence with the following parameters: repetition delay (TR) of 3000 ms, 16 time-echo increments (linearly spaced from 10 to 160 ms), matrix dimension of 256 x 128 and two averages, corresponding to an image acquisition time of 12 min 48 sec. Fourteen continuous slices with slice thickness of 1.0 mm were acquired with a field of view of 3.25 x 2.5 cm2. Quantitative T2-maps were generated from multi-echo, T2-weighted images using an in-house Matlab program. The average T2 of the colon was calculated for each slice. Differences in the mean T2 across all of the images slices were compared using a T-test statistic test.

Caco-2 preparation. Caco-2 cells were cultured in Dulbecco's modified Eagle's minimum essential medium (DMEM, pH 7.4) supplemented with 25 mM glucose, 10% inactivated fetal bovine serum (FBS), 1% penicillinstreptomycin and 1% non-essential amino acid solution. Cells were maintained at 37˚C in a humidified 5% CO2 atmosphere.

Determinations of transepithelial electrical resistance (TEER). Caco-2 cells were grown in the same medium and plated at 1x105 cells/100 µl on Millicell- cell culture inserts (Millipore, Bedford, MA). Cellular TEERs were measured with an electrical resistance system, Millicell-ERS-2 (Merck). Cells with stable TEER readings >500 Ωcm^2 were used. Medium was replaced with either medium containing citrullne 1% and fisetin 100µM dissolved in DMSO or control medium containing DMSO. After 24 hr, 1% DSS (MP Biomedicals; molecular weight 36,000–

50,000 Da) was exposed to apical sides of Caco-2 cell monolayers. Analyses were performed in >5 replicates.

16S rRNA Analysis: Stool samples of 12 weeks old *Asl*$^{f/f}$ and *Villin*^{Cre}*:Asl*$^{f/f}$ mice on arginine free diet since weaning, and *Asl*$^{f/f}$ mice on standard diet were collected and froze in liquid nitrogen. Samples were processed for DNA isolation using MoBio (PowerSoil kit) according to the manufacturer's instructions. The purified DNA from feces was used for PCR amplification and sequencing of the bacterial 16S rRNA gene. Amplicons of ~380 base pairs spanning the variable region 3-4 (V3-4) of the 16S rRNA gene were generated by using designated primers. The PCR products were subsequently pooled in an equimolar ratio, purified (PCR clean kit, Promega), and used for Illumina MiSeq sequencing. Reads were processed using the QIIME (quantitative insights into microbial ecology) analysis pipeline as described (Elinav et al., 2011) version 1.8. Paired-end joined sequences were grouped into operational taxonomic units (OTUs) using the UCLUST algorithm and the GreenGenes database (DeSantis et al., 2006). Sequences with distance-based similarity of 97% or greater over median sequence length of 353 bp were assigned to the same OTU. Analysis was performed at each taxonomical level (phylum to genus and specie level if possible) separately. For each taxon, statistical tests were performed between the different groups. P values was FDR-corrected for multiple hypothesis testing.

References

Becker, C., Fantini, M.C., and Neurath, M.F. (2006). High resolution colonoscopy in live mice. Nat. Protoc. *1*, 2900–2904.

Berger, C.N., Crepin, V.F., Roumeliotis, T.I., Wright, J.C., Carson, D., Pevsner-Fischer, M., Furniss, R.C.D., Dougan, G., Dori-Bachash, M., Yu, L., et al. (2017). Citrobacter rodentium Subverts ATP Flux and Cholesterol Homeostasis in Intestinal Epithelial Cells In Vivo. Cell Metab. *26*, 738–752.e6.

Cohen, S.A., and Michaud, D.P. (1993). Synthesis of a fluorescent derivatizing reagent, 6-aminoquinolyl-N-hydroxysuccinimidyl carbamate, and its application for the analysis of hydrolysate amino acids via high-performance liquid chromatography. Anal. Biochem. *211*, 279–287.

DeSantis, T.Z., Hugenholtz, P., Larsen, N., Rojas, M., Brodie, E.L., Keller, K., Huber, T., Dalevi, D., Hu, P., and Andersen, G.L. (2006). Greengenes, a chimera-checked 16S rRNA gene database and workbench compatible with ARB. Appl. Environ. Microbiol. *72*, 5069–5072.

Elinav, E., Strowig, T., Kau, A.L., Henao-Mejia, J., Thaiss, C.A., Booth, C.J., Peaper, D.R., Bertin, J., Eisenbarth, S.C., Gordon, J.I., et al. (2011). NLRP6 inflammasome regulates colonic microbial ecology and risk for colitis. Cell *145*, 745–757.

Gray, N., and Plumb (2014). A validated method for the quantification of amino acids inmamalian urine.

Iorio, F., Bosotti, R., Scacheri, E., Belcastro, V., Mithbaokar, P., Ferriero, R., Murino, L., Tagliaferri, R., Brunetti-Pierri, N., Isacchi, A., et al. (2010). Discovery of drug mode of action and drug repositioning from transcriptional responses. Proc. Natl. Acad. Sci. *107*, 14621–14626.

Lamb, J., Crawford, E.D., Peck, D., Modell, J.W., Blat, I.C., Wrobel, M.J., Lerner, J., Brunet, J.-P., Subramanian, A., Ross, K.N., et al. (2006). The Connectivity Map: using gene-expression signatures to connect small molecules, genes, and disease. Science *313*, 1929–1935.

Napolitano, F., Sirci, F., Carrella, D., and di Bernardo, D. (2016). Drug-set enrichment analysis: a novel tool to investigate drug mode of action. Bioinforma. Oxf. Engl. *32*, 235–241.

Wirtz, S., Neufert, C., Weigmann, B., and Neurath, M.F. (2007). Chemically induced mouse models of intestinal inflammation. Nat. Protoc. *2*, 541–546.

Zhang, X., Goncalves, R., and Mosser, D.M. (2008). The isolation and characterization of murine macrophages. Curr. Protoc. Immunol. *Chapter 14*, Unit 14.1.

Zigmond, E., Bernshtein, B., Friedlander, G., Walker, C.R., Yona, S., Kim, K.-W., Brenner, O., Krauthgamer, R., Varol, C., Müller, W., et al. (2014). Macrophage-restricted interleukin-10 receptor deficiency, but not IL-10 deficiency, causes severe spontaneous colitis. Immunity *40*, 720–733.

Zwighaft, Z., Aviram, R., Shalev, M., Rousso-Noori, L., Kraut-Cohen, J., Golik, M., Brandis, A., Reinke, H., Aharoni, A., Kahana, C., et al. (2015). Circadian clock control by polyamine levels through a mechanism that declines with age. Cell Metab. *22*, 874–885.

Sup. Figure 1

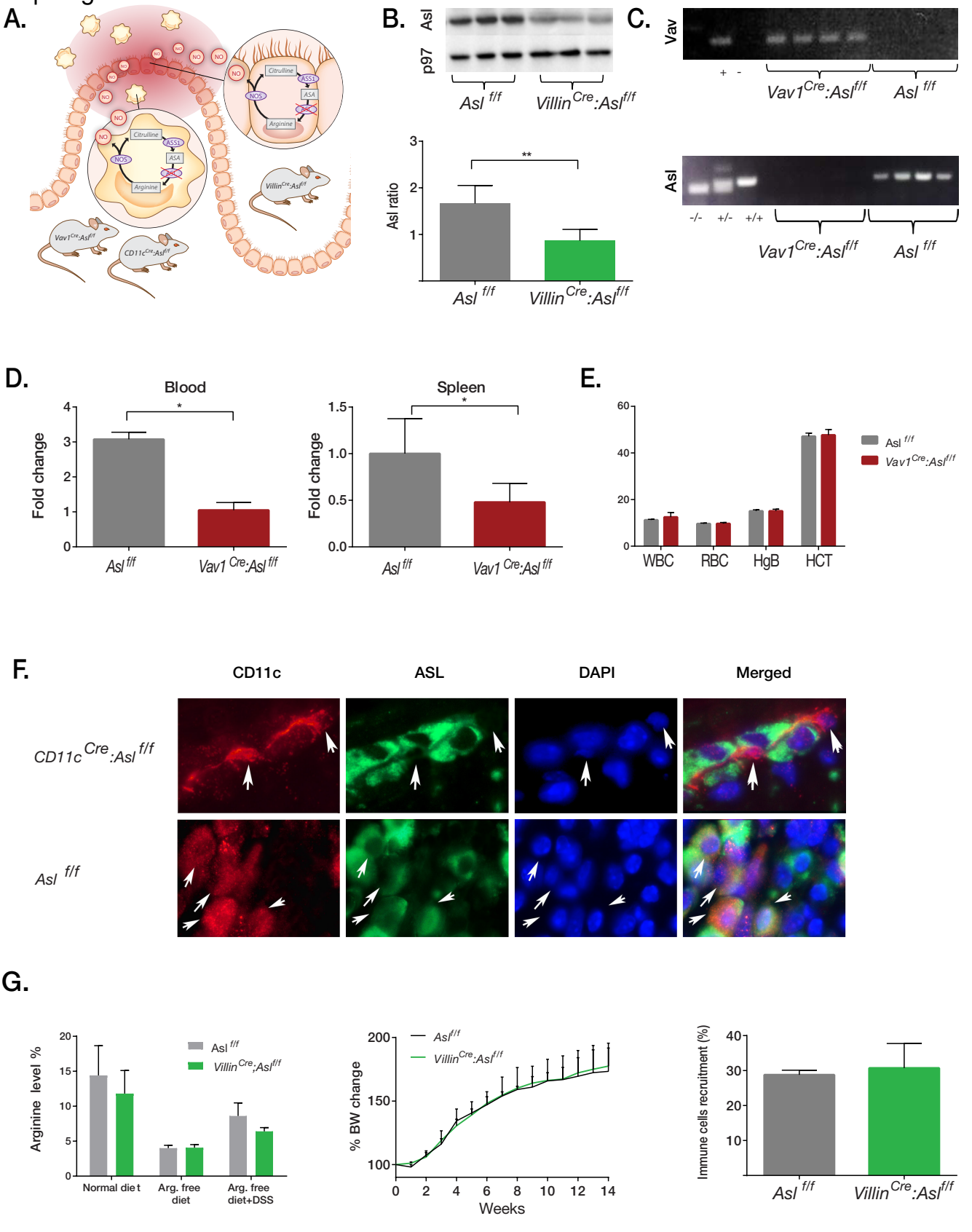
A.
B.
Asl
p97
Asl f/f
Villin Cre:Asl f/f
Asl ratio
**
C.
Vav
+ -
Vav1 Cre:Asl f/f
Asl f/f
Asl
-/- +/- +/+
D.
Blood
Spleen
Fold change
*
E.
WBC
RBC
HgB
HCT
F.
CD11c
ASL
DAPI
Merged
CD11c Cre:Asl f/f
Asl f/f
G.
Arginine level %
Normal diet
Arg. free diet
Arg. free diet+DSS
% BW change
Weeks
Immune cells recruitment (%)

Supplementary Figure 1- Generation of ASL CKO mice and a genetic colitis model. Related to figures 1,2,3 and 4 **(A)** An illustration of the experimental model using mice with deletion of Asl in the hematopoietic system - Vav1Cre: Aslf/f, and CD11cCre:Aslf/f and in mice with deletion of Asl in the epithelial cells - VillinCre:Aslf/f. The magnified cells in circles represent the CKO in enterocytes by VillinCre:Aslf/f (upper right) and the CKO in immune cells in general by VavCre+/- and specifically in macrophages by CD11cCre+/- (lower left). **(B)** A western blot on whole intestinal homogenate showing decreased ASL protein expression in intestine in of neonatal VillinCre:Aslf/f mice as compared to controls. **(C)** A PCR gel of DNA from blood shows expression of Vav Cre but not of Asl in the Vav1Cre: Aslf/f mice; (-/-) complete KO of Asl, (+/-) heterozygous Asl KO and (+/+) wild type Asl expression, (n= 4 in both groups). **(D)** RT PCR showing decreased Asl expression in Vav1Cre: Aslf/f mice' blood (left panel) and spleen (right panel), as normalized to levels of the housekeeping gene Hypoxanthine Phosphoribosyltransferase (HPRT), (n= 3 in each group). **(E)** A complete blood count shows no differences between the Vav1Cre: Aslf/f and control groups. WBC; white blood cells, RBC; red blood cells, HgB; hemoglobin, HCT; hematocrit, (n=6 in each group). **(F)** Immunohistochemistry staining for ASL in CD11c cells showing ASL expression in Aslf/f mice (merged panel), but not in CD11cCre: Aslf/f. Arrows indicating CD11c expression. In red- CD11c, green- ASL, blue – DAPI. **(G)** Plasma arginine levels are similar in VillinCre:Aslf/f and in control mice fed for 10 weeks after weaning with a normal or arginine free diet at baseline or after induction of colitis,(left panel) (n>3 in each group). Arginine deficient diet did not cause growth differences between control and VillinCre:Aslf/f measured over 14 weeks post weaning (middle panel) or in recruitment of CD45+ immune cells to the intestine as determined by FACS (right panel). Statistical analyses were performed using one-way ANOVA, two-way ANOVA, repeated-measures ANOVA or Student's t-test. ; *P <0.05, ** P <0.005.

Sup. Figure 2

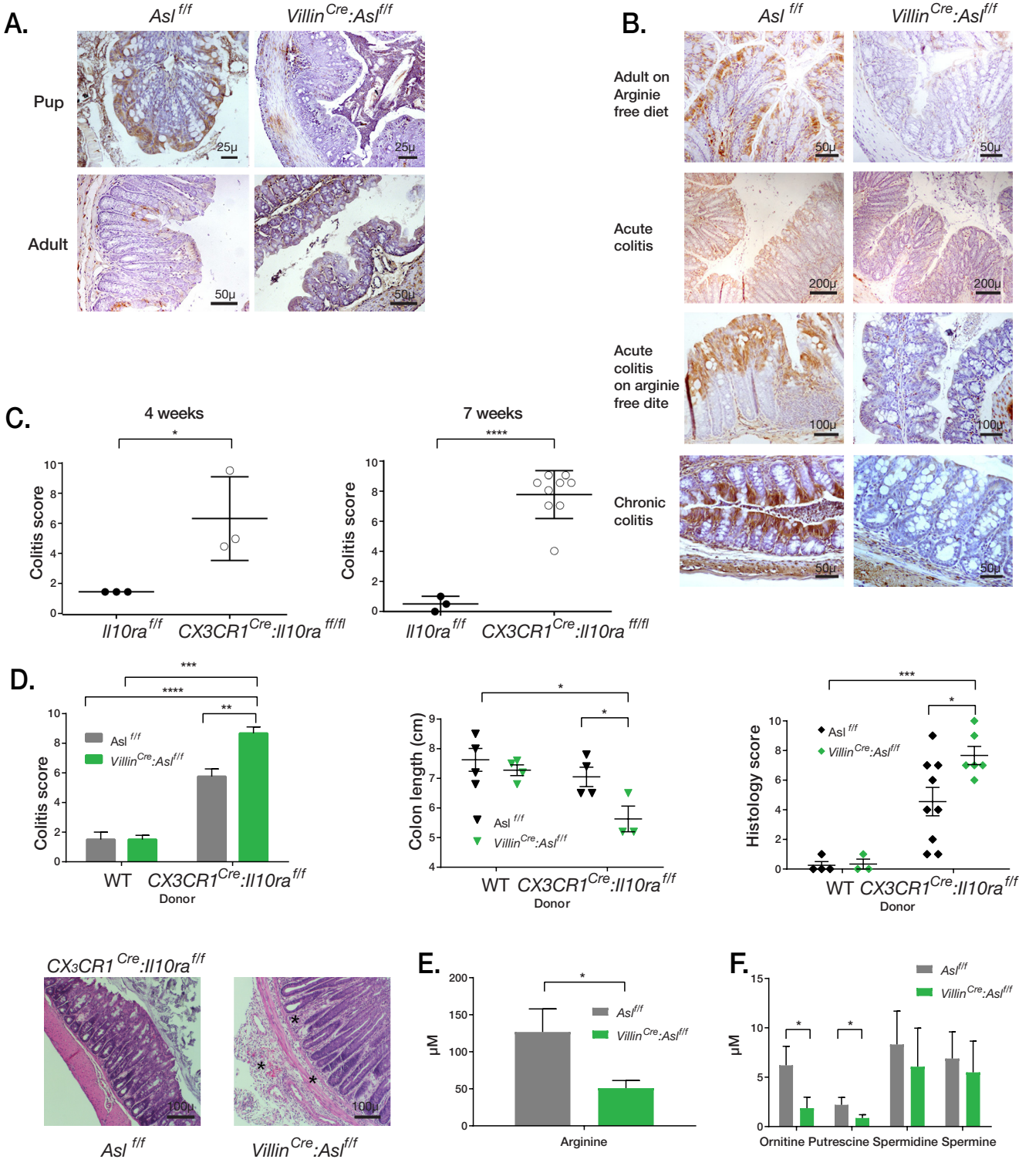
A.
Asl f/f
Villin Cre:Asl f/f
Pup
Adult
25µ
50µ
B.
Asl f/f
Villin Cre:Asl f/f
Adult on Arginie free diet
Acute colitis
Acute colitis on arginie free dite
Chronic colitis
50µ
200µ
100µ
C.
4 weeks
7 weeks
Colitis score
Il10ra f/f
CX3CR1 Cre:Il10ra ff/fl
D.
Asl f/f
Villin Cre:Asl f/f
WT
CX3CR1 Cre:Il10ra f/f
Donor
Colitis score
Colon length (cm)
Histology score
CX3CR1 Cre:Il10ra f/f
Asl f/f
Villin Cre:Asl f/f
E.
µM
Arginine
F.
Ornitine Putrescine Spermidine Spermine

Supplementary Figure 2 - ASL expression levels in enterocytes is state specific. Related to figures 1 and 2. **(A)**. Immunohistochemistry staining for ASS1 showing that ASL expression in the intestine of 10 days old pups decreases in the intestine of adult mice. **(B)** Immunohistochemistry staining shows increased ASL expression in the intestine of control mice when they are fed with arginine free diet for 10 weeks after weaning. Whereas induction of acute colitis per se does not upregulate ASL in the control mice enterocytes, an increased expression is seen during colitis when fed with arginine-free diet. An increase in ASL in control mice enterocytes was seen also after induction of the chronic colitis model in which the colitis was induced for 2 months **(C)** Lethally irradiated wild type animals that received a bone marrow (BM) graft from CX3CR1Cre:Il10rafl/fl developed colitis as indicated by colitis score at 4 weeks and 7 weeks after BM implantation, as compared to control chimeras. **(D)** Colitis was induced by bone marrow (BM) transplantation from wildtype (WT) or CX3CR1Cre:Il10ra fl/fl donors, to lethally irradiated VillinCre:Aslf/f and to control Aslf/f mice. While no colitis signs were detected in mice receiving WT BM, VillinCre:Aslf/f mice transplanted with CX3CR1Cre:Il10ra fl/fl BM, had increased severity of colitis compared to control mice, as demonstrated by a higher endoscopic colitis score 5 weeks after BM transplantation (left panel) (n>3 in each group); shorter colon length (middle panel), and by a higher histologic score due to increased infiltration, edema and ulcers (right panels), representative colon cross section stained with H&E showing extensive edema and cellular infiltration in the VillinCre:Aslf/f mice compare to controls, (left lower panel) (n>3 in each group). Asterisks indicate areas with edema and increased cellular infiltration. **(E)** Liquid chromatography–mass spectrometry (LC/MS) measurement of arginine shows significantly reduced levels in the enterocytes of VillinCre:Aslf/f mice as compared to arginine levels in control mice on day 11 after colitis induction **(F)** Following colitis induction, polyamine measurements using LC/MS show significantly reduced levels of ornithine and putrescine in enterocytes of VillinCre:Aslf/f mice as compared to control mice, while no differences were observed in the spermidine and spermine levels. Statistical analyses were performed using one-way ANOVA, two-way ANOVA, repeated-measures ANOVA or Student's t-test; *P <0.05, ** P <0.005, ***P <0.0005, ****P <0.00005.

Sup. Figure 3

A.

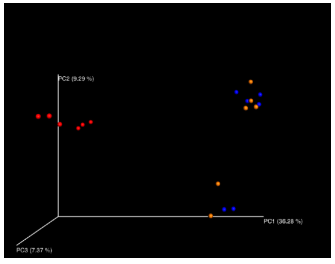

Weighted

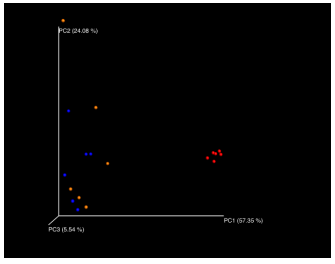

Unweighted

$Asl^{f/f}$

$Asl^{f/f}$ Arg.free diet

$Villin^{cre}$;$Asl^{f/f}$ Arg. free diet

B.

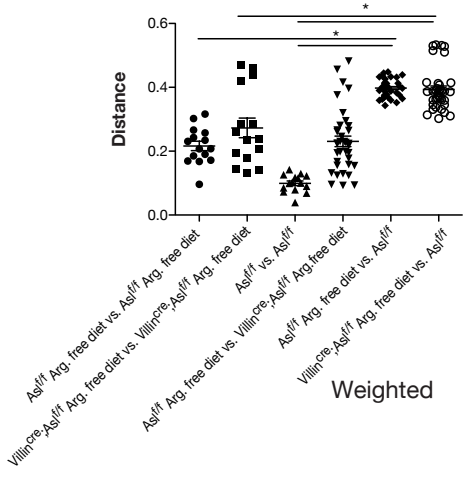

Weighted

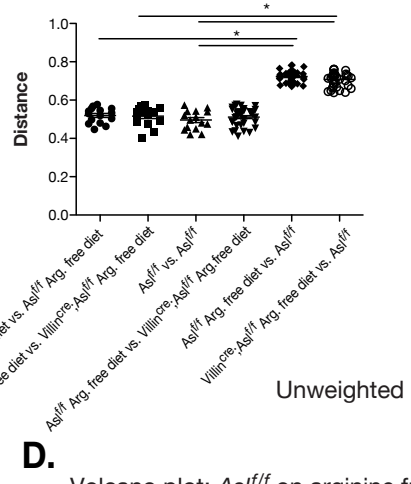

Unweighted

C.

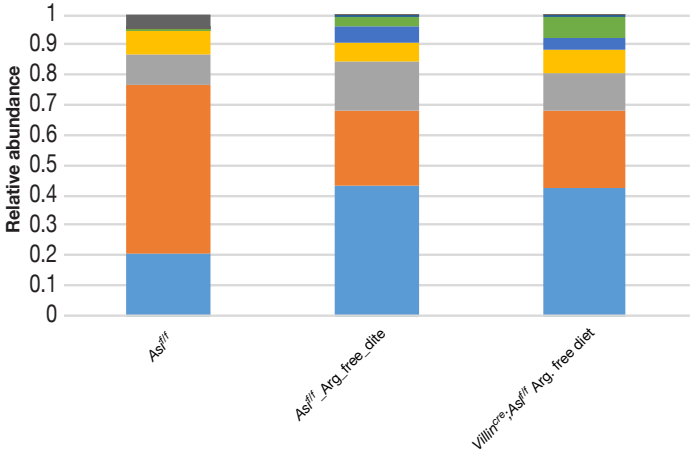

D.

Volcano plot: $Asl^{f/f}$ on arginine free diet vs. $Villin^{Cre}$:$Asl^{f/f}$ on arginine free diet

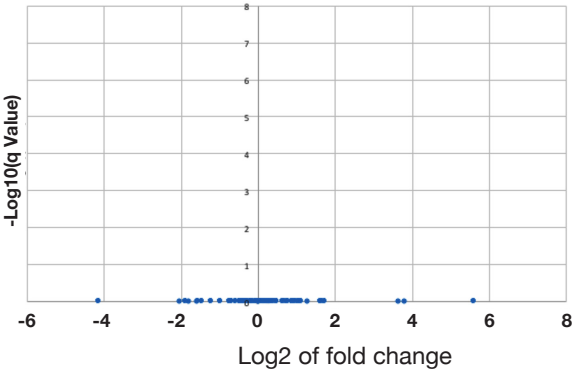

k__Bacteria;p__Firmicutes

k__Bacteria;p__Bacteroidetes

k__Bacteria;p__Proteobacteria

k__Bacteria;p__Verrucomicrobia

k__Bacteria;p__Actinobacteria

k__Bacteria;p__Deferribacteres

Unassigned;Other

k__Bacteria;p__Tenericutes

k__Bacteria;p__Cyanobacteria

Supplementary figure 3: ASL expression levels in the enterocytes does not affect the microbiome. Related to figures 1 and 2. Stool samples of 12 weeks old Aslf/f and VillinCre:Aslf/f mice on arginine free diet since weaning, and of Aslf/f mice on standard diet, were collected for 16S rRNA sequencing analyses. No separation between Aslf/f and VillinCre:Aslf/f mice on arginine free diet are seen, as shown by 3D weighted and un-weighted Principal coordinates analysis (PCoA) of UniFrac distances of 16S rRNA sequencing **(A)**, by quantification of the UniFrac distances of 3D weighted and un-weighted Principal coordinates analysis (PCoA) of 16S rRNA, by 1-way ANOVA with Bonferroni posttest **(B)**, by the averages of Phylum bacterial relative abundance in stool samples **(C)**, and by Volcano plot for bacteria taxa abundance **(D)**. N=6 in each group, * $P<0.05$.

Sup. Figure 4

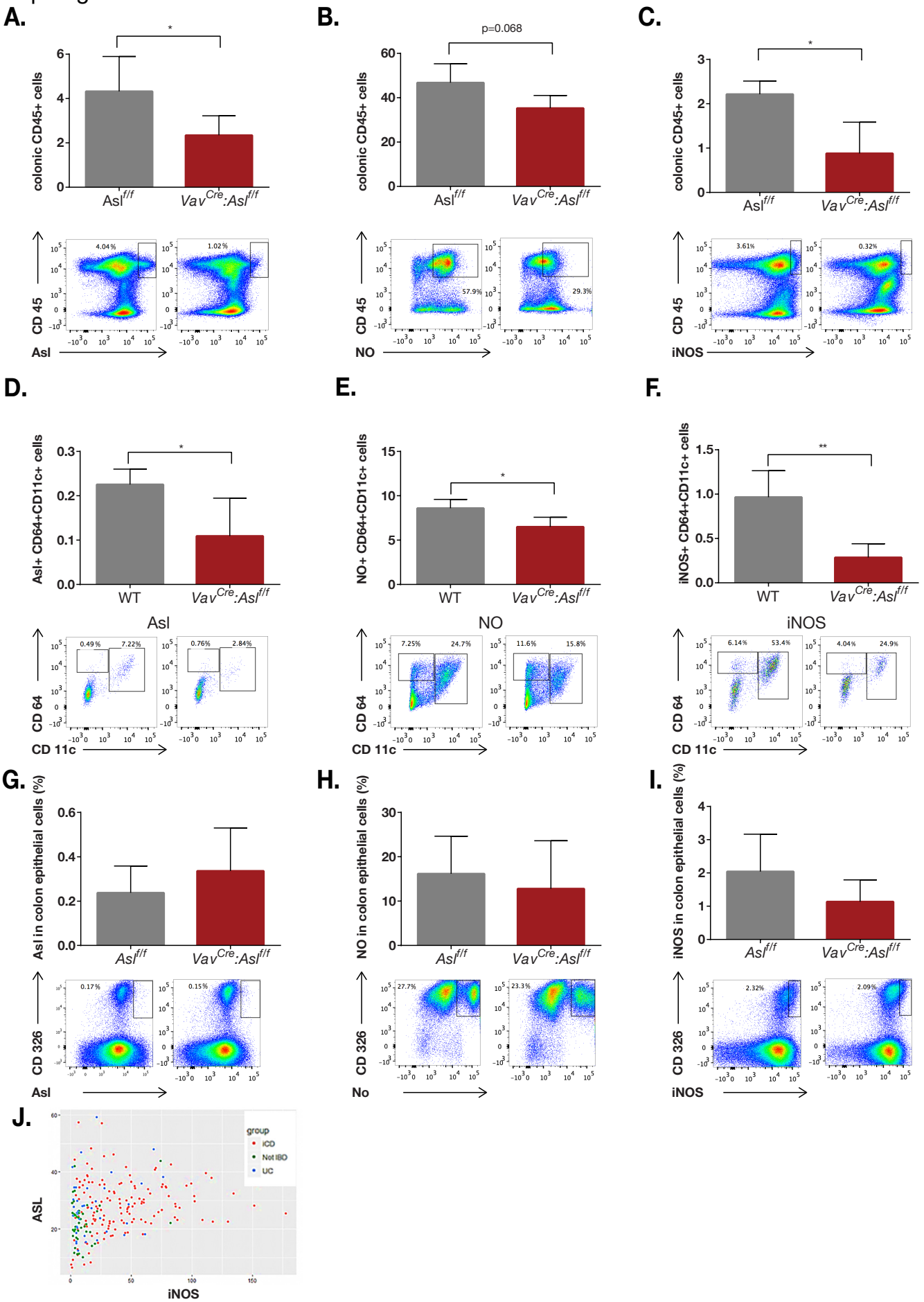
A.
B.
C.
colonic CD45+ cells
Asl^f/f
Vav^Cre:Asl^f/f
p=0.068
4.04%
1.02%
57.9%
29.3%
3.61%
0.32%
CD 45
Asl
NO
iNOS
D.
E.
F.
Asl+ CD64+CD11c+ cells
NO+ CD64+CD11c+ cells
iNOS+ CD64+CD11c+ cells
WT
Asl
NO
iNOS
0.49%
7.22%
0.76%
2.84%
7.25%
24.7%
11.6%
15.8%
6.14%
53.4%
4.04%
24.9%
CD 64
CD 11c
G.
H.
I.
Asl in colon epithelial cells (%)
NO in colon epithelial cells (%)
iNOS in colon epithelial cells (%)
0.17%
0.15%
27.7%
23.3%
2.32%
2.09%
CD 326
No
J.
ASL
iNOS
group
iCD
Not IBD
UC

Supplementary Figure 4- Cell specific ASL deficiency correlates with decreased NO production. Related to figure 3 and 4. FACS analysis of colon cells from Vav1Cre: Aslf/f and from control Aslf/f mice, after colitis induction by DSS shows a significant increase in the levels of ASL, NO and iNOS in CD45+ colon immune cells of the control group but not in the Vav1Cre: Aslf/f mice **(A-C)**, as well as in the CD64+, CD11c+ macrophages. **(D-F)**, however no differences in these parameters are seen in CD326 colon enterocytes **(G-I)**, ($n \geq 4$ in each group). Statistical analyses were performed using Student's t-test; *P <0.05, ** P <0.005. **(J)** ASL expression correlates with iNOS in colon of patients with and without IBD, analysis of GEO dataset- GSE57945 ID: 200057945, (R=0.27; pV= 2.612e-05).

Sup. Figure 5

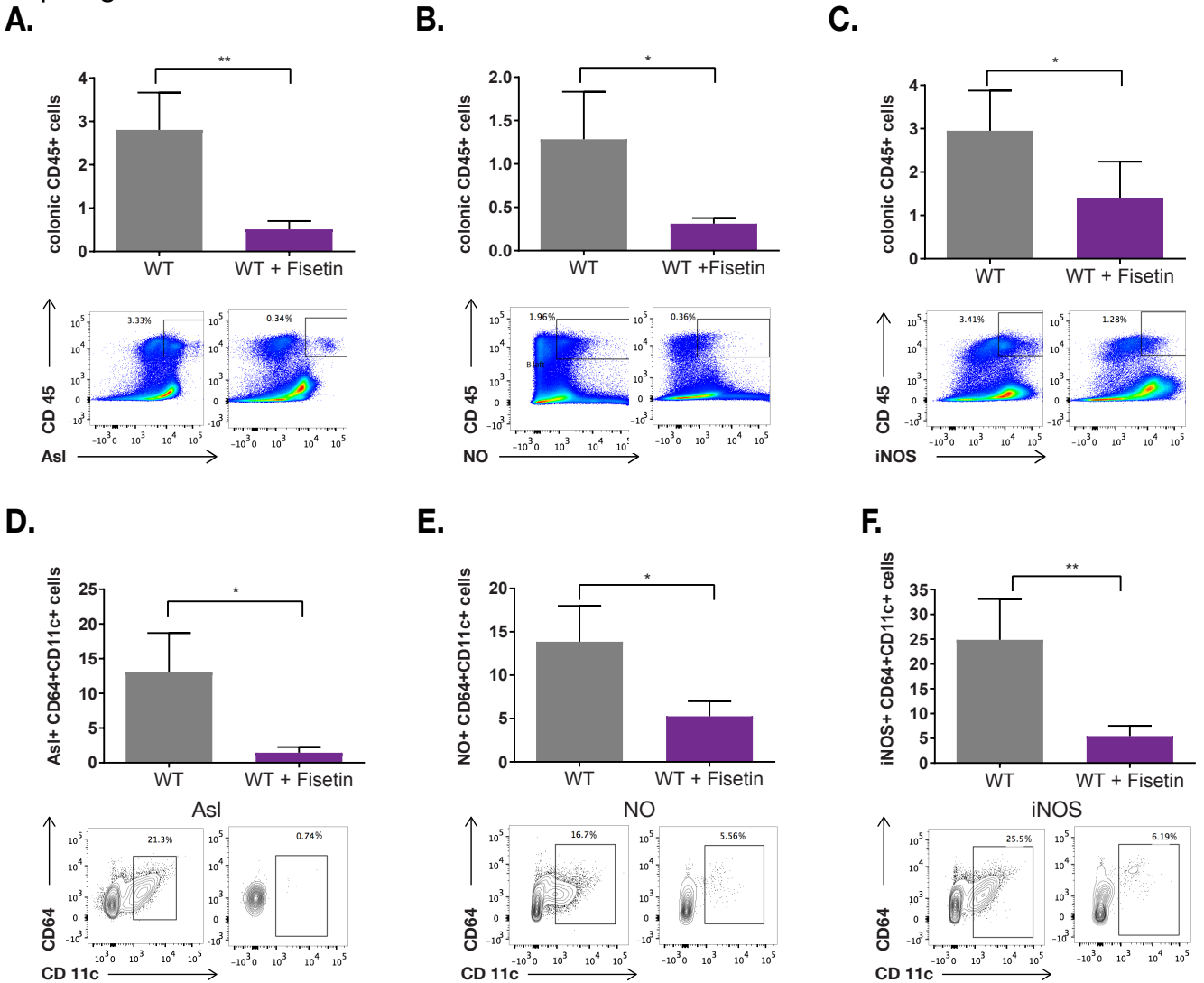
A.
B.
C.
D.
E.
F.
colonic CD45+ cells
WT
WT + Fisetin
WT +Fisetin
CD 45
AsI
NO
iNOS
3.33%
0.34%
1.96%
0.36%
3.41%
1.28%
AsI+ CD64+CD11c+ cells
NO+ CD64+CD11c+ cells
iNOS+ CD64+CD11c+ cells
CD64
CD 11c
21.3%
0.74%
16.7%
5.56%
25.5%
6.19%

Supplementary Figure 5 - Fisetin does not increase NO levels in intestinal immune cells. Related to figure 6. FACS analysis of colon cells from mice treated with fisetin vs control after colitis induction shows decrease in ASL, NO and iNOS expression levels in CD45+ immune system cells after fisetin treatment **(A-C)**, as well as in the CD64+, CD11c+ macrophages **(D-F)**, (n=4 in each group). Statistical analyses were performed using Student's t-test; *P <0.05, ** P <0.005.

Table 1

Gene	Up	Down
ASL	alsterpaullone	Prestwick-1083
	copper_sulfate	baclofen
	dexamethasone	butirosin
	fisetin	chlorpropamide
		clofazimine
		doxepin
		isosorbide
		pinacidil
		pyridoxine
		thiocolchicoside
		trazodone
ASS1	azacitidine	cefotaxime
	fisetin	celecoxib
	staurosporine	

Supplementary Table 1: FDA approved small molecules that affect ASL and ASS1 expression levels. Related to figure 6 and 7. The table summarizes all FDA approved small molecules that upregulate or downregulate ASL and ASS1 expression levels in response to FDA approved small molecular screen.